Available online at www.sciencedirect.com
SCIENCE DIRECT
Molecular Phylogenetics and Evolution 39 (2006) 512–528
MOLECULAR PHYLOGENETICS AND EVOLUTION
www.elsevier.com/locate/ympev

Phylogeny and biogeography of Altingiaceae: Evidence from combined analysis of five non-coding chloroplast regions

Stefanie M. Ickert-Bond [a,*], Jun Wen [b,c]

[a] *Field Museum, Department of Botany, 1400 S. Lake Shore Dr., Chicago, IL 60605-2496, USA*
[b] *Smithsonian Institution, Department of Botany, United States National Herbarium and National Museum of Natural History, MRC-166, P.O. Box 37012, Washington, DC 20013-7012, USA*
[c] *Laboratory of Systematic and Evolutionary Botany and Herbarium, Institute of Botany, Chinese Academy of Sciences, Beijing 100093, People's Republic of China*

Received 31 August 2005; revised 6 December 2005; accepted 7 December 2005
Available online 24 January 2006

Abstract

The Altingiaceae consist of ~15 species that are disjunctly distributed in Asia and North America. The genus *Liquidambar* has been employed as a biogeographic model for studying the Northern Hemisphere intercontinental disjunctions. Parsimony and Bayesian analyses based on five non-coding chloroplast regions support that (1) *Liquidambar* is paraphyletic; (2) the temperate *Liquidambar acalycina* and *Liquidambar formosana* are nested within a large tropical to subtropical Asian clade; (3) *Semiliquidambar* is scattered in the eastern Asian clade and is of hybrid origin involving at least two maternal species: *L. formosana* and *L. acalycina*; and (4) the eastern North American *Liquidambar styraciflua* groups with the western Asian *Liquidambar orientalis*, but is highly distinct from other lineages. Biogeographically, our results demonstrate the complexity of biogeographic migrations throughout the history of Altingiaceae since the Cretaceous, with migration across both the Bering and the North Atlantic land bridges.

Keywords: Biogeography; Phylogeny; Altingiaceae; Divergence times; *Liquidambar*; Hamamelidaceae

1. Introduction

Altingiaceae Horan. (the sweet gums) are a family of ~15 species in three genera, *Liquidambar* L., with four to five species, *Altingia* Noronha, with six to eight species, and *Semiliquidambar* H.-T. Chang, with ~three species. The family shows a classic Asian/North American intercontinental biogeographic disjunction. The Altingiaceae are most species rich in Asia, with two genera, *Altingia* and *Semiliquidambar* endemic to tropical and subtropical Asia. The four species of *Liquidambar* are disjunctly distributed in eastern Asia (2 spp.), western Asia (1 sp.), and eastern North America to Central America (1 sp.). Some controversies concern the delimitation of *Liquidambar styraciflua* L., with the southern populations in Mexico and Central America formerly designated as a separate species, *Liquidambar macrophylla* Oersted (Sosa, 1978). Most workers, however, recognize only one species in the New World that exhibits considerable variation in leaf and infructescence size (e.g., Meyer, 1993).

Altingiaceae are anemophilous trees with pentaporate pollen, unisexual flowers that lack a perianth, woody infructescences, and flowers with several stamens each aggregated into staminate capitula (Ferguson, 1989). The presence of resin ducts associated with vascular bundles of stems, leaves, and floral organs is found throughout the Altingiaceae, but is also present in Hamamelidaceae *s. str.* (Bogle, 1986). The Altingiaceae have been discussed extensively through studies of pollen morphology (Chang, 1959, 1964; Zavada and Dilcher, 1986), floral anatomy (Bogle, 1986; Wisniewski and Bogle, 1982), wood anatomy

* Corresponding author. Fax: +1 312 665 7158.
E-mail address: sbond@fieldmuseum.org (S.M. Ickert-Bond).

1055-7903/$ - see front matter © 2005 Elsevier Inc. All rights reserved.
doi:10.1016/j.ympev.2005.12.003

(Greguss, 1959; Huang, 1986; Metcalfe and Chalk, 1950; Moll and Janssonius, 1914; Rao and Purkayastha, 1972; Reinsch, 1890; Tang, 1943; Tippo, 1938) and relationships in Hamamelidaceae *s. l.* (Endress, 1989a,b,c, 1993; Endress and Igersheim, 1999; Endress and Stumpf, 1990). Based on a gynoecium with two carpels and a stigma with multicellular papillae, Altingiaceae have generally been placed in Hamamelidaceae *s. l.*(Chang, 1973, 1979; Cronquist, 1981; Endress and Igersheim, 1999). Endress (1993) concluded that the Exbucklandiaceae are a link between the Hamamelidaceae *s. str.* and Altingiaceae. Similarly, Hufford and Crane (1989) based on a cladistic analysis of morphology also showed that Exbucklandioideae, Rhodoleioideae, and Altingioideae form a subclade within Hamamelidaceae *s. l.* Recent molecular studies have shown this assemblage to be polyphyletic and support recognizing Altingiaceae and Hamamelidaceae *s. str.* as distinct families in the Saxifragales within a larger rosid clade (APG, 2003; Chase et al., 1993; Magallón et al., 1999; Soltis et al., 2000). The order Altingiales, including Altingiaceae and Rhodoleiaceae, was recognized and included in the superorder Trochodendranae along with the order Trochodendrales (Doweld, 1998).

Within *Liquidambar*, allozyme (Hoey and Parks, 1991, 1994) and phylogenetic analyses of DNA sequence data (Li et al., 1997a,b; Li and Donoghue, 1999; Shi et al., 1998) suggest a sister-species relationship between the North American *L. styraciflua* L., and the western Asian *Liquidambar orientalis* Mill. While none of these studies addresses the monophyly of *Liquidambar*, several studies have documented the paraphyly of the genus (Shi et al., 1998, 2001; Wen, 1999). Two sections were traditionally recognized within *Liquidambar*: sect. *Liquidambar* and sect. *Cathayambar* Harms (Harms, 1930). Harms (1930) used the presence of "Borsten" ("setae" sensu Bogle, 1986), in the inflorescences and infructescences of *Liquidambar formosana* as the defining character for his section *Cathayambar*. The remaining species (*L. orientalis* and *L. styraciflua*) were placed in sect. *Euliquidambar* (=sect. *Liquidambar*) and were stated as lacking these structures. When *Liquidambar acalycina* was described (Chang, 1979), it was placed in sect. *Liquidambar* along with *L. orientalis* and *L. styraciflua*. *Liquidambar formosana* from Asia is highly distinct from others due to numerous long spinose phyllomes (=setae of Bogle, 1986) between adjacent fruits, which are lacking from the eastern North American and the western Asian species (Ickert-Bond et al., 2005). The other eastern Asian species, *L. acalycina* overlaps with *L. formosana* in distributional range, but replaces it at elevations above 1200 m. Unlike other *Liquidambar* species, *L. acalycina* shares several characters with *Altingia* (Ickert-Bond et al., 2005; Pigg et al., 2004), particularly seeds that are lacking the characteristic distal wing of *Liquidambar*, but instead have a circular flange around the seed.

Altingia is distributed in tropical and subtropical Asia and comprises about six morphologically variable species (Table 1) with controversial species circumscriptions. Leaves in this genus range from ovate to obovate in shape, coriaceous to chartacous and vary widely in size from 5 cm in length in *A. gracilipes* Hemsl. to more than 12 cm in *A. yunnanensis* Rehder and Wilson. Two sections have been recognized: sect. *Altingia* Noronha, including *A. chinensis*, *A. obovata*, *A. yunnanensis*, *A. poilanei*, and *A. excelsa*, has large spheroidal heads with numerous fruits, while sect. *Oligocarpa* H.-T. Chang, including *A. gracilipes* and *A. siamensis* has no more than nine fruits per infructescence which is smaller, and hemispheroidal to turbinate in shape (Chang, 1979; Ferguson, 1989). Morphological analysis of infructescences in this genus is currently underway (S.M. Ickert-Bond, K.B. Pigg, and J. Wen, in prep.)

Semiliquidambar from South and eastern China has ~three species (Figs. 1 and 2): *S. cathayensis* H.-T. Chang from Fujian, Guangdong, Guangxi, Guizhou, Hainan, and Jiangxi, *S. caudata* H.-T. Chang from Fujian and Zhejiang provinces, and *S. chingii* (Metcalf) H.-T. Chang from Fujian, Guangdong, and Jiangxi province. *Semiliquidambar cathayensis* occupies a large area overlapping with *Liquidambar* and *Altingia* in South China (Chang, 1962, 1979; Ferguson, 1989). Leaves of *Semiliquidambar* combine characters from *Altingia* (simple leaves with camptodromous venation) and *Liquidambar* (palmately-lobed leaves with actinodromous venation). *Semiliquidambar* was proposed to be a possible intergeneric hybrid between *Liquidambar* and *Altingia* (Bogle, 1986; Ferguson, 1989; Shi et al., 2001).

The fossil record of Altingiaceae dates back to the Late Cretaceous, but its Neogene record is remarkably robust. The earliest evidence for Altingiaceae fossils are recently described Late Cretaceous mesofossils from New Jersey and the Allon flora of central Georgia (Herendeen et al., 1999; Zhou et al., 2001). Although these fossils cannot be assigned to a modern genus, they show that spherical infructescences composed of biloculate fruits were among some of the earliest eudicot infructescences. A morphological cladistic analysis of Altingiaceae (Ickert-Bond et al., 2005) that focused on intergeneric relationships in *Liquidambar*, found support for *Microaltingia* Zhou, Crepet, and Nixon from the Late Cretaceous of New Jersey, belonging to the stem lineage of Altingiaceae. An additional globose infructescence that has been assigned to the Altingiaceae is the genus *Steinhauera* Presl., an infructescence that is known from many Eocene localities of Europe (Mai, 1968). Leaves, infructescences, and seeds recognized as *Liquidambar* also appear from the Eocene to the Pliocene in western North America, Europe, and Asia (Ferguson, 1989; Manchester, 1999; Pigg et al., 2004; Wolfe, 1973). The greatest occurrence of the Altingiaceae is in the Miocene, where compressed leaves and fruits are commonly found in localities in Asia, Europe, and North America (Manchester, 1999; Pigg et al., 2004). The European record extends only into the Pliocene, while the group has continued to persist in western and eastern Asia and eastern North America.

To date, no molecular phylogenetic study of Altingiaceae based on extensive sampling has been conducted. Two studies focused solely on interspecific relationships in *Liquidambar* (Li et al., 1997a,b; Li and Donoghue, 1999).

Table 1
Plant material and GenBank accession numbers

Species	Locality	Voucher	*trn*L-*trn*F	*psa*A-*ycf3*	*rps*16	*trn*S-*trn*G	*Trn*G	*rbc*L
Liquidambar								
L. acalycina	U.S.A.: Washington, Seattle, Washington Arboretum, cult.	*WA 85-90*	DQ352215	DQ352246	DQ352280	DQ352312	DQ352344	—
L. acalycina	China: Hubei, Lichuan	*Wen 8146-11*	DQ352216	DQ352247	DQ352281	DQ352313	DQ352345	DQ352380
L. formosana	Vietnam: Mt. Bavi National Park, on road to summit	*Ickert-Bond 1291*	DQ352220	DQ352251	DQ352285	DQ352317	DQ352349	DQ352384
L. formosana	China: Hainan, Lingshui Co., Diaoluo Mtn. National Forest Park	*Ickert-Bond 1363*	DQ352221	DQ352252	DQ352286	DQ352318	DQ352350	—
L. macrophylla	Mexico: Veracruz, Banderilla	*Ickert-Bond 1390*	DQ352218	DQ352249	DQ352283	DQ352315	DQ352347	DQ352382
L. macrophylla	Mexico: Hidalgo, Rd. to Huathutla, before ciudad Ocotillo	*Ickert-Bond 1383*	DQ352219	DQ352250	DQ352284	DQ352316	DQ352348	—
L. orientalis	U.S.A.: Washington, Seattle, Washington Arboretum	*WA 1386-56*	DQ352222	DQ352253	DQ352287	DQ352319	DQ352351	—
L. orientalis	Turkey, Muğla, between Köyceğiz and Kavak	*Aksoy 5203*	DQ352223	DQ352254	DQ352288	DQ352320	DQ352353	—
L. orientalis	Turkey, Isparta, Sütçüler, Karacaören	*Aksoy 5204*	DQ352224	DQ352255	DQ352289	DQ352321	DQ352352	DQ352383
L. styraciflua	U.S.A.: Alabama, Clay Co.	*Wen 7169*	DQ352217	DQ352248	DQ352282	DQ352314	DQ352346	DQ352381
Semiliquidambar								
S. cathayensis	China: Guangdong prov., Rd. to Hunan	*Ickert-Bond 1322*	DQ352200	DQ352232	DQ352265	DQ352297	DQ352329	—
S. cathayensis	China: Guangdong prov., Rd. to Hunan	*Ickert-Bond 1323*	DQ352201	DQ352233	DQ352266	DQ352297	DQ352330	—
S. cathayensis	China: Zhejiang,	*Ickert-Bond 1376*	DQ352199	DQ352231	DQ352264	DQ352296	DQ352328	—
S. caudata	China: Hainan, Lingshui Co., Diaoluo Mtn. National Forest Park	*Ickert-Bond 1367*	DQ352258	DQ352230	DQ352263	DQ352295	DQ352327	—
Altingia								
A. sp.	Vietnam, Kon Tum province, Kong Plong distr., Mieu municipality	*WP 227*	DQ352214	DQ352245	DQ352279	DQ352311	DQ352343	—
A. chinensis	China: Hong Kong, Shin Mun Country Parks	*Ickert-Bond 1261*	DQ352202	DQ352234	DQ352267	DQ352299	DQ352331	DQ352376
A. cf.*chinensis*	Vietnam: Sa Pa, near Ta Pinh village	*Ickert-Bond 1294*	DQ352203	DQ352235	DQ352268	DQ352300	DQ352332	—
A. excelsa	Thailand: Kow Yai National Park	*J. F. Maxwell s.n.*	DQ352225	DQ352256	DQ352290	DQ352322	DQ352354	—
A. excelsa	Indonesia: Western Java, Cibodas	*E. A. Widjaja. s.n.*	DQ352226	DQ352257	DQ352291	DQ352323	DQ352355	DQ352374
A. gracilipes	China: Hong Kong, Pat Sin Leng Country Park	*Ickert-Bond 1272*	DQ352205	DQ352237	DQ352270	DQ352302	DQ352334	—
A. gracilipes	China: Guangdong prov., Heping Co., Reshui	*Ickert-Bond 1344*	DQ352206	DQ352238	DQ352271	DQ352303	DQ352335	—
A. gracilipes	China: Zhejiang prov., Taishun	*Ickert-Bond 1379*	DQ352207	DQ352239	DQ352272	DQ352304	DQ352336	DQ352379
A. obovata	China: Hainan, Wanning Co.	*Ickert-Bond 1356_5*	DQ352209	DQ352241	DQ352274	DQ352306	DQ352338	DQ352377
A. obovata	China: Hainan, Ledong Co., Jiangeng Natural Reserve	*Ickert-Bond 1372*	DQ352208	DQ352240	DQ352273	DQ352305	DQ352337	—
A. poilanei	Vietnam: Sa Pa, near Ta Pinh village	*Ickert-Bond 1296*	DQ352210	DQ352259	DQ352275	DQ352307	DQ352339	—
A. siamensis	Cambodia: Bokor National Park, Pokopville waterfall	*Ickert-Bond 1280*	DQ352213	DQ352244	DQ352278	DQ352310	DQ352342	—
A. siamensis	Cambodia: Bokor National Park, Pokopville waterfall	*Ickert-Bond 1281*	DQ352212	DQ352243	DQ352277	DQ352309	DQ352341	DQ352375
A. yunnanensis	Vietnam: Sa Pa, near Ta Pinh village	*Ickert-Bond 1295*	DQ352211	DQ352242	DQ352276	DQ352308	DQ352340	DQ352378
Outgroup								
Corylopsis pauciflora	U.S.A.: Illinois, Clark Co., Chicago, UIC campus, cult.	*Ickert-Bond 1400*	DQ352358	DQ352363	—	—	—	DQ352369
Daphniphyllum			AB178610	AF377997	—	—	—	L01901
Disanthus cercidifolius			AF147467	n.a.	—	—	—	AF060709
Exbucklandia tonkinensis	China: Hong Kong, Lantau Island	*Ickert-Bond 1269*	DQ352198	DQ352229	DQ352262	DQ352294	DQ352326	DQ352372
Hamamelis mollis	China: Jiangxi, Lushan, Shanbaoshu	*Wen 5519*	DQ352357	DQ352362	—	—	—	DQ352367
Hamamelis virginiana	USA: Virginia, Giles Co.	*Wen 6229*	DQ352196	DQ352227	DQ352260	DQ352292	DQ352324	DQ352368
Loropetalum chinense	China: Jiangxi prov.	*Ickert-Bond 1325*	DQ352359	DQ352364	—	—	—	DQ352370
Mylilaria laosensis			n.a.	AF304544	—	—	—	AF062001
Rhodoleia championii	Vietnam: Sa Pa, road to Ta Pinh	*Ickert-Bond 1293*	DQ352197	DQ352228	DQ352261	DQ352293	DQ352325	DQ352373
Tetrathyrium subcordatum	China: Hong Kong, Shin Mun Country Parks	*Ickert-Bond 1264*	DQ352360	DQ352365	—	—	—	DQ352371

All voucher specimens are deposited at the Field Museum Herbarium (F).

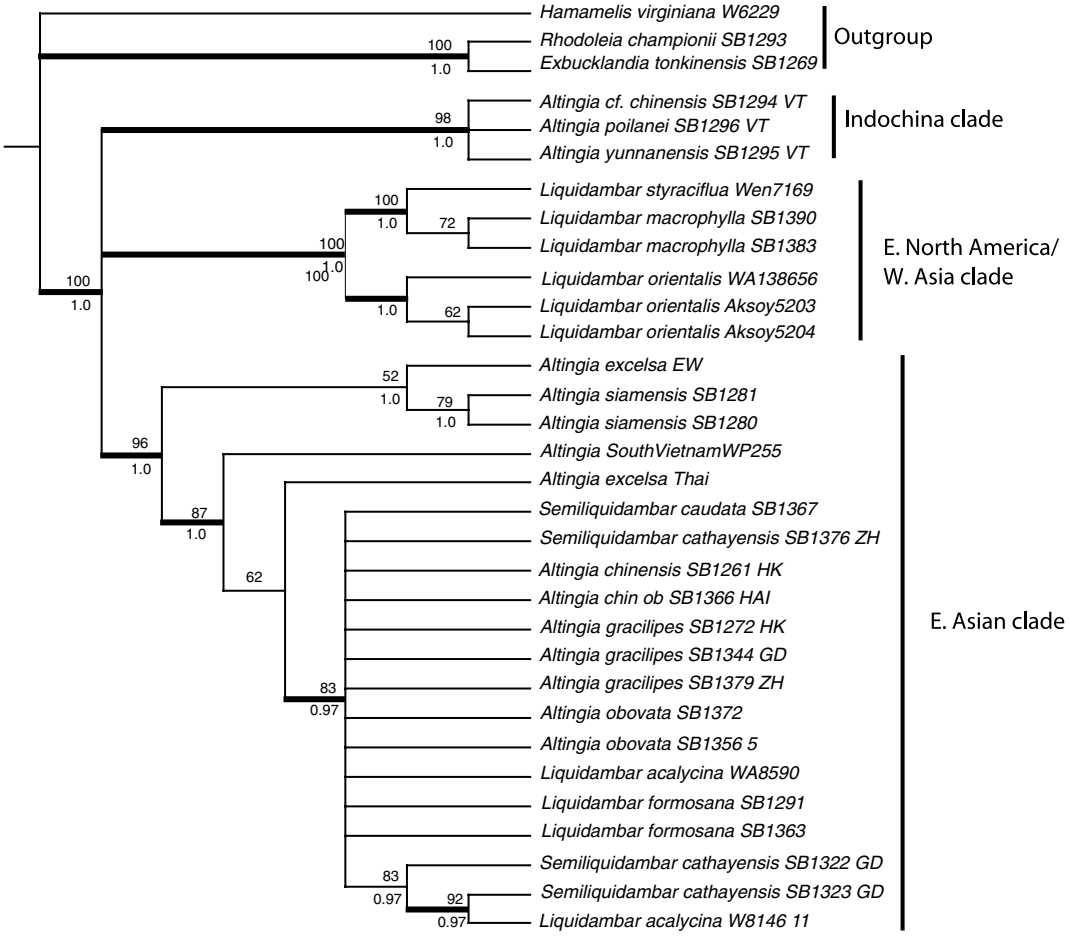

Fig. 1. Phylogeny of *Altingiaceae* based on parsimony analysis of combined analysis of five non-coding *cp*DNA sequence data. Tree is the strict consensus of 1000 (maxtrees) equally parsimonious trees of length 820 steps, $CI = 0.967$, $RI = 0.946$, derived from heuristic analyses (random addition sequence, TBR branch swapping, MULTREES in effect). Bootstrap values are given above branches for clades resolved in strict consensus, below the branches are Bayesian posterior probabilities.

An attempt at further resolving relationships within Altingiaceae was made by Shi et al. (2001), who showed *Liquidambar* to be paraphyletic and a possible hybrid origin for *Semiliquidambar*. Additionally, several unresolved phylogenetic and morphological questions remain unanswered. They include the following: (1) What are the detailed phylogenetic relationships among and within the genera *Liquidambar*, *Altingia*, and *Semiliquidambar*? (2) Will the previously reported paraphyly of *Liquidambar* be supported with expanded taxon sampling and additional markers? (3) Is *Altingia* monophyletic? (4) Are species of *Altingia* with a wide geographic distribution monophyletic? (5) Does further molecular evidence support the intergeneric hybrid origin of *Semiliquidambar*? (6) When did the split between north temperate and subtropical elements occur in Altingiaceae?

To resolve species relationships within Altingiaceae, we have generated chloroplast sequences from five non-coding regions: the *trn*L-*trn*F intergenic spacer (IGS), the *psa*A-*ycf3* IGS, the *rps*16 intron, the *trn*S-*trn*G IGS, and the *trn*G intron (Huang and Shi, 2002; Oxelman et al., 1997; Shaw et al., 2005; Taberlet et al., 1991). We also included *A. siamensis* from Cambodia and *A. yunnanensis* from Vietnam and southwestern China which are not sampled in the Shi et al. (2001) study, and a larger number of accessions to represent the biogeographic diversity of certain widespread species, recently collected in Cambodia, China, and Vietnam. In addition to parsimony analysis, we also employ a Bayesian approach that allows efficient analysis of datasets while employing a complex nucleotide substitution model in a parametric statistical framework (Huelsenbeck et al., 2001; Larget and Simon, 1999).

2. Materials and methods

2.1. Taxon sampling

A total of 39 accessions representing the 26 species accepted here (Table 1) were sequenced for the *trn*L-*trn*F IGS, the *psa*A-*ycf3* IGS, the *rps*16 intron, the *trn*S-*trn*G IGS, and the *trn*G intron. *Hamamelis*, *Exbucklandia*, and *Rhodoleia* were used as outgroups, because these taxa were found basal within Hamamelidaceae *s. l.* and Exbucklandioideae are considered a link between the Altingiaceae and the

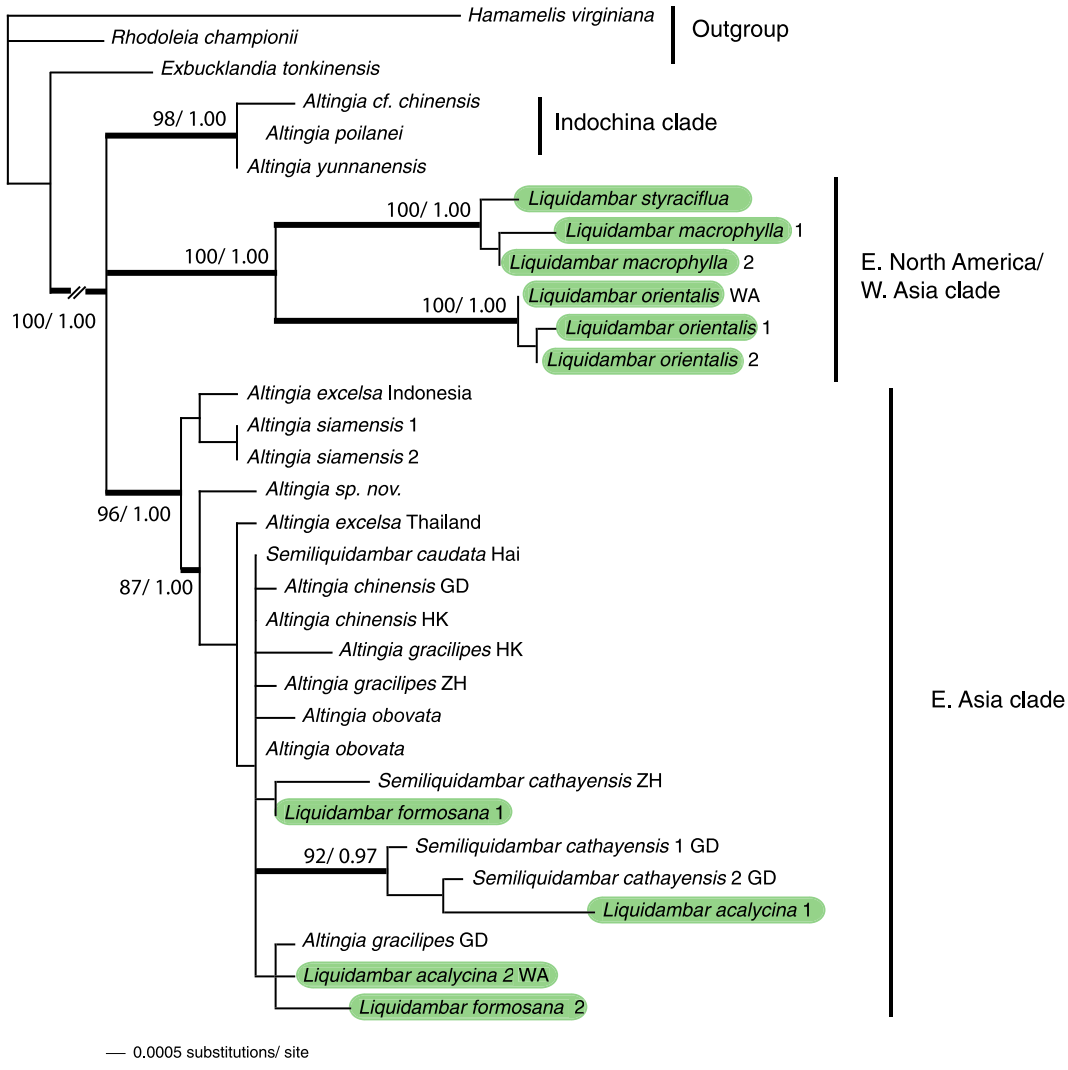

Fig. 2. Branch lengths estimates based on maximum likelihood analyses of combined analysis of *cp*DNA data of Altingiaceae. Phylogram is one of 14 trees ($-\ln L = 9927.72$) derived from maximum likelihood analyses showing rates of substitution under K81uf + I model of substitution evolution. *Note*. Break in branch lengths for the OG at left, and *Liquidambar* taxa with gray boxes.

Hamamelidaceae (Endress, 1993). These taxa are similar to Altingiaceae in their absence of ejecting fruits and pluri-to multiovulate carpels with only the lowermost one or two reaching maturity (Endress, 1989b, 1993; Hufford and Crane, 1989). Other members of Hamamelidaceae *s. l.* have ejecting fruits with single ovules (Endress, 1989b, 1993).

Since several fossil constraints used in our analysis of divergence time lied outside Altingiaceae, we included sequences from a number of closely related taxa that represent major lineages within hamamelidaceous eudicots (Table 1). Substitution rate heterogeneity among genetically divergent clades was a concern when using fast-evolving non-coding markers such as the *rps*16 intron, the *trn*S-*trn*G IGS, and the *trn*G intron, and precluded alignment between outgroups and the ingroup when estimating divergene times. To achieve unambiguous alignment and rooting in this broader sampling approach we relied on *rbc*L sequences combined with sequences from the *trn*L-*trn*F IGS and the *psa*A-*ycf3* IGS.

2.2. DNA extraction, amplification, and sequencing

Fresh or silica-dried material was available for most taxa. Genomic DNAs were isolated using DNA extraction kits (Qiagen, Alameda, California). The *trn*L-*trn*F IGS was amplified using primers of Taberlet et al. (1991). The *psa*A-*ycf3* intergenic spacer (IGS) was amplified with the primers PG1f and PG2r of Huang and Shi (2002). The *rps*16 intron was amplified with primers rpsF and rpsR2 of Oxelman et al. (1997). The entire *trn*S-*trn*G region was amplified with primers trnS and 3′trnG, with additional internal sequencing primers 5′trnG2G and 5′trnG2S (Shaw et al., 2005). Due to large strings of mononucleotides, additional internal sequencing primers trnG_Al_R510 (5′ CTATGTCAGCTTTTCTGTC 3′), trnS_Al_F594 (5′ ACTGGCCCTCTTTTTTGA 3′), and trnS_Al_R500 (5′ GGAATGGAAATAGCCCCTCTTC 3′) were designed. The *rbc*L region was amplified following Bremer et al. (1995), while some sequences of outgroup taxa were available in GenBank (Table 1).

The PCR amplifications were performed in 25 μl reactions containing 10–100 ng genomic DNA, 0.2 mM deoxyribonucleotide triphosphates (equimolar), 0.5 U *Taq* polymerase, oligonucleotide primers at 0.5 μM, and Mg^{2+} at 1.5 mM. The DNA sequences were amplified for the *trn*L-*trn*F IGS, the *psa*A-*ycf3* IGS, the *rps*16 intron, and *rbc*L with the following conditions: 38 cycles of denaturation (94 °C, 20 s), annealing (50 °C, 30 s), and extension (72 °C, 40 s), and concluding with a final extension (72 °C, 15 min). The *trn*S-*trn*G IGS and the *trn*G intron region were amplified following protocol 1 as outlined in Shaw et al. (2005) with primer annealing and chain extension occurring at 66 °C. Sequences were run in a low melt agarose gel, and the gel containing the required fragments were cut and treated with gelase to digest the gel. Sequencing of both strands was done on an ABI 3730 Genetic Analyzer using ABI Big Dye TM v. 3.1. PCR profile of sequencing was 25 cycles of 96 °C for 1 min, 96 °C for 10 s, 50 °C for 5 s, and 60 °C for 4 min.

Sequences were assembled into contigs using Sequencher, version 4.1 (Gene Codes, Ann Arbor, Michigan). Sequence alignments were initially made in ClustalX (Jeanmougin et al., 1998) and edited manually.

2.3. Phylogenetic analyses

The aligned data were analyzed using the programs PAUP* 4.0 beta10 (Swofford, 2002) and MrBAYES 3.0 (Huelsenbeck and Ronquist, 2001) using both the parsimony and maximum likelihood (Swofford et al., 1996) and Bayesian approaches (Huelsenbeck et al., 2001; Larget and Simon, 1999). Base frequencies were empirically determined, and the transition: transversion (K) ratio and gamma shape parameter (Γ) were estimated on MP trees under the model of sequence evolution, chosen using results from MODELTEST version 3.06 (Posada and Crandall, 1998). A partitioned Bayesian analysis of the total five noncoding dataset was implemented by applying the previously determined models of each data partition (Table 1). The goal of partitioning is to divide the data into sequence regions that have evolved under different models of evolution to reduce systematic error and infer better resolved or supported relationships (Brandley et al., 2005; Nylander et al., 2004). Initial runs were conducted with starting with random, neighbor-joining, or minimum evolution trees to check the number of simultaneous MCMC chains necessary to avoid being trapped on local optima. Subsequently, the MCMC was run for 2,000,000 generations with 12 incrementally heated chains, starting from random trees and sampling one out of every 100 generations. A majority-rule consensus tree was calculated with PAUP* from the last 18,001 out of the 20,001 trees sampled. Log-likelihood scores of sample points were plotted against generation time using TRACER 1.2 (http://evolve.zoo.ox.ac.uk/software.html?id=tracer) and determined that stationarity was achieved when the log-likelihood values of the sample points reached a stable equilibrium value (Huelsenbeck and Ronquist, 2001). The first 2000 trees (burn-in) were excluded to avoid trees that might have been sampled prior to convergence of the Markov chains. The posterior probability of each topological bipartition was estimated by the frequency of these bipartitions across all 18,001 trees sampled. Internodes with posterior probabilities $\geqslant 95\%$ were considered statistically significant.

We also used a Bayesian approach to examine heterogeneity in phylogenetic signal between the five data partitions (Buckley, 2002; Buckley et al., 2002; Kauff and Lutzoni, 2002; Reeder, 2003). For each region, and for the concatenated analyses, the set of topologies reaching the 0.95 posterior probability was estimated. Then, we determined whether the topology of the combined analysis was within the 0.95 posterior intervals of each *cp*DNA region. If the topology was within the 0.95 posterior intervals for any of the five *cp*DNA regions, no conflict existed, and we could assume that the concatenated topology could have given rise to the observed data and the data partitions could be combined. If conflict was evident, than the particular partition had evolved along another topology, and combining the data partitions might be potentially misleading (Huelsenbeck and Bull, 1996).

Maximum parsimony (MP) was also used to reconstruct phylogenetic relationships. All characters were unordered, equally weighted, and gaps treated as missing data. Parsimony analyses were conducted using heuristic search methods and employed all addition sequence options (simple, closest, random addition sequences) in combination with tree-bisection reconnection (TBR) branch-swapping and the MulTrees option, which saves all minimal trees. Individual analysis of the *trn*L-*trn*F IGS, the *trn*S-*trn*G IGS, the *psa*A-*ycf3* IGS, the *rps*16, and the *trn*G intron were performed. Since no conflict was evident it was assumed that the five datasets were congruent. A strict consensus tree was generated and support for individual clades was estimated using non-parametric bootstrap methods (Felsenstein, 1985). Bootstrap proportions (BP) were obtained from 2000 replicates of heuristic searches as described above (1000 random addition sequences, TBR branch swapping, and MulTrees selected). Maximum likelihood analyses (ML) were conducted with the combined chloroplast dataset using PAUP* to compare with results from parsimony analyses. A single tree derived from parsimony or neighbor joining analysis was used as a starting tree for a heuristic search (addition sequence "ASIS") with TBR branch swapping and MULTREES in effect. A hierarchical likelihood ratio test (Modeltest 3.04 PPC; Posada and Crandall, 1998) was used to select the nucleotide substitution models and parameters for ML searches.

Three hypothesized phylogenetic relationships of Altingiaceae reported in recent publications (Table 2) were tested as null hypotheses using a MCMC tree sampling procedure as described above. For the hypothesis testing, a run, as previously specified, was performed with the same settings as in the estimation of the phylogeny using the combined dataset.

Table 2
Probabilities of phylogenetic null hypotheses being correct

Null hypothesis	Bayesian probalility[a]	SOWH probability[b]
Monophyly of *Liquidambar*	0.025*	0.001**
Monophyly of *Liquidambar*, subgenus *Liquidambar*	0.025*	0.001**
Monophyly of *Altingia*	0.001*	0.001**

[a] Each test is based on a Bayesian MCMC tree sample of 2000 trees.
[b] Each test is based on 100 simulated data sets using Seq-Gen.
* Probabilities significant at <0.05.
** Probabilities significant at >0.001.

Two thousand trees at the equilibrium state per null hypothesis were used from this analysis. The probability of the null hypothesis being correct was calculated by counting the presence of this topology in the MCMC sample (Lewis, 2001; Lumbsch et al., 2004). The frequency of trees in the MCMC sample agreeing with each null hypothesis was calculated using the filter command in PAUP* with the constraint describing the null hypothesis. To evaluate alternative phylogenetic hypotheses thoroughly we also performed a parametric bootstrap and an *a posteriori* significance test (i.e., SOWH test; Goldman et al., 2000; Huelsenbeck and Bull, 1996; Pereira and Baker, 2004). We first prepared a null distribution for the difference in likelihood scores using a parametric re-sampling approach by simulating 100 sequence alignments under the null hypothesis topology with the program Seq-Gen version 1.2.7 (Rambaut and Grassly, 1997). Differences in log likelihoods of the original data and the alternative phylogenetic hypotheses (Table 2) were compared with the null distribution of differences in log likelihoods over the replicates for the two trees.

2.4. Divergence time estimation

To obtain age estimates that could rely on a broad range of fossil calibrations we employed the *rbc*L gene, which has been sequenced for many species of lower eudicots (Table 1) and which is unambiguously alignable, as well as two non-coding (*trn*L-*trn*F IGS, *psa*A-*ycf3* IGS) chloroplast regions. Maximum likelihood methods were employed to infer tree topologies and branch lengths for this combined dataset.

Rate constancy was tested with a likelihood ratio test (Felsenstein, 1988). Where the molecular data departed from clock-like evolution, we used two relaxed-clock approaches to infer divergence times from the chloroplast data: (1) the penalized likelihood (PL; Sanderson, 2002, 2003) and (2) the Bayesian relaxed molecular clock approach (BRC; Thorne and Kishino, 2002). We used several fossils as calibration points (Fig. 3) to infer both absolute ages of clades as well as maximum or minimum age constraints (Sanderson, 1997). The stem lineage of Altingiaceae was constrained to be minimally 90 mya old, based on fossil inflorescences, fruits and pollen of *Microaltingia* (Zhou et al., 2001). The split between Hamamelideae and Corylopsideae was constrained to be minimally 85 mya old based on the fossil flowers of *Androdecidua endressii* Magallón, Herendeen, and Crane (Magallón et al., 2001), while the age of *Corylopsis* was constrained to be minimally 50 mya old based on fossil leaves of *Corylopsis reedae* Radtke, Pigg, and Wehr (Radtke et al., 2005). Within Altingiaceae we constrained the divergence of the clade (*L. acalycina* (*L. formosana–A. obvata*)) from the rest of the eastern Asian clade to be minimally 15.6 mya old based on the western North American Middle Miocene *L. changii* Pigg, Ickert-Bond, and Wen (Pigg et al., 2004). To estimate the standard errors associated with divergence times estimated with the PL method, we used a parametric bootstrapping strategy similar to that in Davis et al. (2002). We simulated 100 datasets on the maximum likelihood tree with Seq-Gen version 1.2.7 (Rambaut and Grassly, 1997), imported those 100 simulated datasets into PAUP and used them to generate new maximum likelihood trees, and finally estimated the divergence times on each of the new trees (using r8s), and the resulting node ages were used to calculate the variance on the estimates obtained from the original tree.

The Bayesian time estimating procedure we followed is divided into three different steps and programs, and is described in more detail in a step-by-step manual available at http://www.plant.ch/software.html. In the first step, we used the 'baseml' program of PAML ver. 3.14 (Yang, 1997) and the F84 + G model (Kishino and Hasegawa, 1989) to estimate base frequencies, transition/transversion rate kappa, and the alpha shape parameter (five categories of rates). Then, by using these parameters, we estimated the maximum likelihood of the branch lengths of the rooted evolutionary tree together with a variance–covariance matrix of the branch length estimates by using the program *Estbranches* (Thorne et al., 1998). The maximum-likelihood scores obtained in *Baseml* and *Estbranches* were then compared to determine if both approaches were able to optimize the likelihood. *Multidivtime* (Thorne and Kishino, 2002) was used to approximate the posterior distributions of substitution rates and divergence times by using a multivariate normal distribution of estimated branch lengths and by running a MCMC procedure following data-dependent settings in the multidivtime control file. The following prior distributions were used in these analyses: 100 mya ($SD = 50$ mya) for the expected time between tip and root if there were no constraints; 0.08 ($SD = 0.04$) substitutions per site per million year for the rate of the root node; 0.02 ($SD = 0.02$) for the parameter that determines the magnitude of autocorrelation per million years; and 100 mya for the largest value of the time unit between the root and the tips. We repeated each analysis twice to assure that Markov chains were long enough to converge.

3. Results

3.1. Size and structure of individual and combined datasets

Detailed information on both individual data partitions and combined datasets is given in Table 3. Multiple sequence

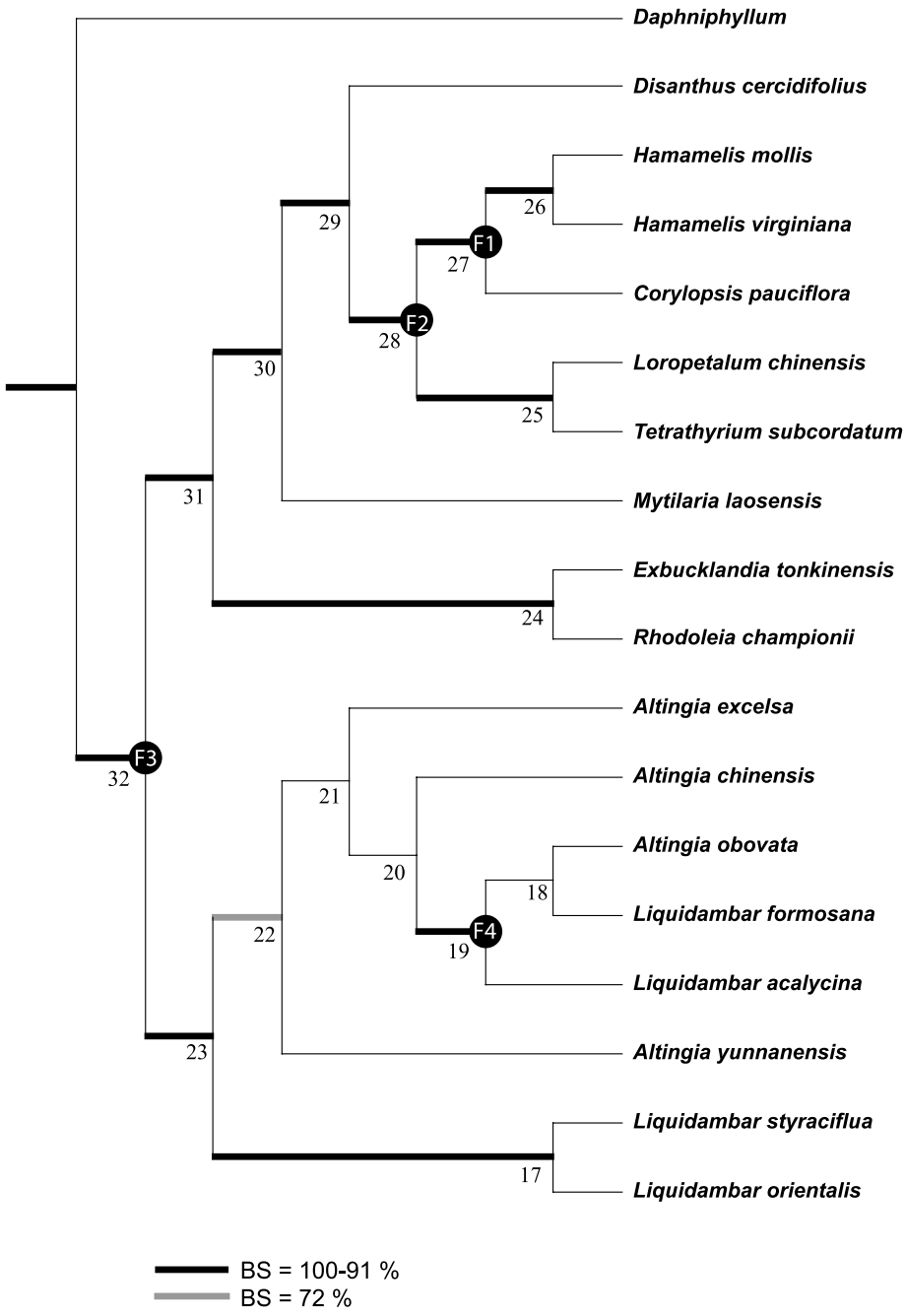

Fig. 3. Strict consensus tree of nine MP trees of combined coding (*rbc*L) and non-coding (*trn*L-*trn*F and *psa*A-*ycf3*-IGS) chloroplast data of Altingiaceae. Numbers below branches are clade names used in Table 4. Numbers at the nodes in black circles correspond to calibration points used in the estimation of divergence times ($F_1 = 49$–50 mya-*Corylopsis reedae*, $F_2 = 85$ mya-*Androdecidua*, $F_3 = 90$ mya-*Microaltingia*, and $F_4 = 15.6$ mya-*Liquidambar changii*).

alignment was straightforward for all the *trn*L-*trn*F, *psa*A-*ycf3* IGS, the *rps*16 intron, and *rbc*L, but proved to be more difficult for the intergenic spacer between *trn*S and *trn*G and the *trn*G intron, due to the large number of AT rich regions. A total number of 22 and 16 characters were excluded for these last two partitions respectively. Among the five individual partitions the percentage of informative characters were highest in the *trn*G-*trn*S IGS (8.91 %) and in the *trn*L-*trn*F IGS (5.42 %), while the remaining three regions were similar in the percentage of informative characters (~4.5%). The chloroplast datasets used to generate phylogenetic relationships were complete, while the dataset for divergence time estimation lacks sequences of *Mytilaria* for the *trn*L-*trn*F IGS and of *Disanthus cercidifolius* for the *psa*A-*ycf3* IGS, due to the unavailability of materials.

3.2. Congruence among partitions

The Bayesian approach for testing incongruence indicates that the ML topology obtained from the concatenated analysis lies within the 0.95 posterior intervals for each of the five *cp*DNA regions (data not shown). This is

Table 3
Characteristics of *cp*DNA datasets and resulting trees of Altingiaceae (excluding uninformative characters)

	cpDNA region					Combined
	*trn*L-*trn*F IGS	*psa*A-*ycf3* IGS	*rps*16 intron	*trn*S-*trn*G IGS	*trn*G intron	
Aligned length	1033	830	860	862	662	4246
Number of characters excluded	—	—	—	20	24	44
Number of variable sites	100	79	68	364	121	505
Total no. of parsimony-informative characters[a] (%)	56 (5.42)	38 (4.58)	39 (4.53)	75 (8.91)	29 (4.54)	237 (5.58)
Within Altingiaceae	9 (0.87)	12 (1.44)	11 (1.28)	14 (1.66)	14 (2.19)	60 (1.41)
Within *Liquidambar*	6 (0.58)	10 (1.22)	7 (0.81)	13 (1.54)	8 (1.25)	44 (1.04)
Mononucleotide repeats	10-13	—	—	11–17	9–21	—
Mean GC content (%)	0.37	0.82	0.79	0.82	1.31	0.92
Pairwise divergences[b] (%)						
Within Altingiaceae	0.35 (0.00–0.62)	0.19 (0.00–1.18)	0.48 (0.00–0.95)	0.77 (0.00–1.16)	0.62 (0.00–4.10)	0.48 (0.00–1.22)
Within *Liquidambar*	0.38 (0.00–0.73)	0.85 (0.00–1.19)	0.51 (0.00–0.84)	0.92 (0.00–1.39)	1.20 (0.00–2.75)	0.57 (0.00–1.22)
No. of trees	1082	8	3	10000	10000	6
No. of steps	107	83	71	414	139	410
CI	0.991	0.976	0.986	0.976	0.950	0.973
RI	0.992	0.980	0.986	0.915	0.915	0.955
Model selected by AIC[c]	TrN + I	K81uf	TIM	K81uf	TVM + I	K81uf + I
Number of nodes with BS > 70%	3	6	5	5	4	6

[a] Percentage of total number of characters.
[b] Based on uncorrected *p* values.
[c] Akaike Information Criterion in Modeltest.

consistent with the hypothesis that the each of the partitions examined evolved along the same underlying topology, and that data can be combined (Bull et al., 1993). Previous studies have documented the increase in resolving power for combined datasets if the data partitions share the same evolutionary history (Buckley et al., 2002; Simoes et al., 2004).

The likelihood parameters in the sample had the following average values (±one standard deviation): base frequencies $\pi(A) = 0.326$ (0.001), $\pi(G) = 0.159$ (±0.001), $\pi(T) = 0.337$ (±0.001), $\pi(C) = 0.178$ (±0.001), rate matrix r(GT) = 1 (±0.0), r(CT) = 2.146 (±0.009), r(CG) = 0.738 (±0.005), r(AT) = 0.575 (±0.003), r(AG) = 2.459 (±0.010), r(AC) = 0.957 (±0.005), and the gamma shape parameter $\alpha = 1.007$ (±0.040).

3.3. Phylogenetic reconstruction

The strict consensus tree of 1000 sampled trees (Fig. 1), when rooted with *Hamamelis* shows a strongly supported Altingiaceae (posterior probability, pp 1.0). Furthermore three distinct clades are highly supported (pp 1.0), (1) a *L. styraciflua* and *L. orientalis* clade, (2) a clade of three accessions from South Vietnam, *Altingia cf. poilanei*, *A. yunnanensis*, and *A. cf. chinensis*, and (3) clade containing the remaining taxa. Within this larger highly supported clade (pp 1.0, BP = 96%) a clade of *A. excelsa* from Indonesia and *A. siamensis* from Cambodia diverges at the base sister to a well supported clade (pp 1.0, BP = 87%) composed of five species of *Altingia,* two species of *Liquidambar* and four accessions of *Semiliquidambar*. Within this large southeast Asian clade only one more clade is resolved. In this well-supported clade (pp 0.97, BP = 87%), two accessions of *Semiliquidambar cathayensis* are well supported as sister to *L. formosana* (pp 0.97, BP = 92%). Comparison of results from parsimony and maximum likelihood analyses (Figs. 1, 2) are largely congruent with respect to overall topology and branch lengths. It is noteworthy, that the partitioned Bayesian analysis showed very slightly improved posterior probabilities, but also inferred a slightly more resolved phylogeny (data not shown) than the one inferred from fully combined data into a single analysis (Fig. 1). In particular the partitioned Bayesian analysis recovered two additional clades within the large southeast Asian clade, which were not inferred in the single partition analysis. One well supported clade is composed of *Semiliquidambar* and two accessions of *L. formosana* (pp 0.99), while the other clade groups *L. acalycina* as sister to *A. gracilipes* (pp 0.90). The two additional clades within the large southeast Asian clade were also recovered in the ML analysis but without support (Fig. 2).

Since the three commonly recognized genera of Altingiaceae are not distinct in the strict consensus tree, we explored whether our data have sufficient phylogenetic signal to significantly reject alternative topologies that may be present in suboptimal trees not represented in the consensus tree. We therefore performed Bayesian hypothesis testing as well as parametric bootstrapping and an a posteriori SOWT test (Table 2), but all alternative hypotheses were rejected by both approaches.

3.4. Divergence time estimates

Clock-like evolution is rejected based on χ^2 values (df = 21, $P < 0.00001$, CV = 60.7). During ML analyses to infer tree topologies and branch lengths for the combined dataset of *rbc*L, the *trn*L-*trn*F IGS, and the *psa*A-*ycf3* IGS chloroplast regions, several clades collapsed and produced

zero-length branches. Zero-length terminal branches were removed from each phylogram before estimating divergence times (Magallón and Sanderson, 2005), since both BRC and PL methods will fail if zero-length branches occur in the topology. Cross validation under PL found a smoothing parameter of 100 to be optimal for the combined chloroplast data.

During Bayesian divergence time estimation, we constrained the stem lineage of Altingiaceae to minimally 90 mya as well as using multiple simultaneous constraints from the ingroup (*Liquidambar changii*) and several outgroups (see Section 2, *Divergence Time Estimation*). Of biogeographic interest, the Bayesian estimation yielded an age of 39 mya (with a 95% credibility interval of 26–54 mya) for the divergence between the *L. styraciflua–L. orientalis* clade and the large eastern Asian clade of *L. acalycina–L. formosana–Altingia*, while the penalized likelihood method yielded an age of 22.70 mya for this divergence (Figs. 4 and 5, Table 4). The age of the intercontinental disjunction between *L. styraciflua* and *L. orientalis* was determined to be 23 mya (credibility interval: 4–43 mya) in the Bayesian divergence time estimation, while the penalized method estimated an age of 10.91 mya for the *L. styraciflua/L. orientalis* divergence (Figs. 4 and 5, Table 4). For detailed results on other nodes outside Altingiaceae see Table 4.

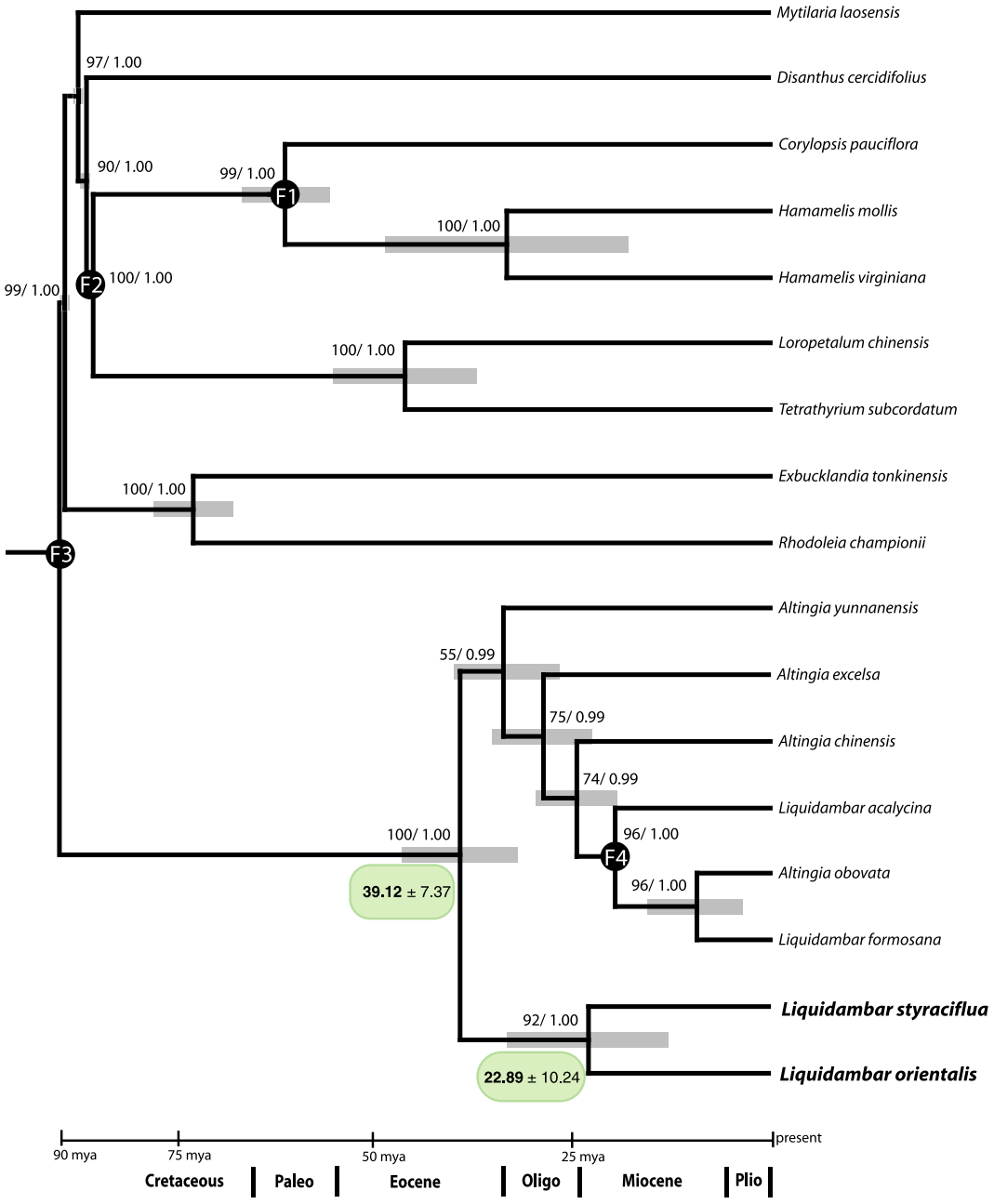

Fig. 4. Chronogram of the maximum likelihood (ML) tree from combined analysis of *rbc*L, *trn*L-*trn*F, and *psa*A-*ycf3*-IGS data of Altingiaceae. Branch lengths transformed via Markov chain Monte Carlo (MCMC) in Bayesian time estimation. Gray boxes reflect 95% confidence intervals.

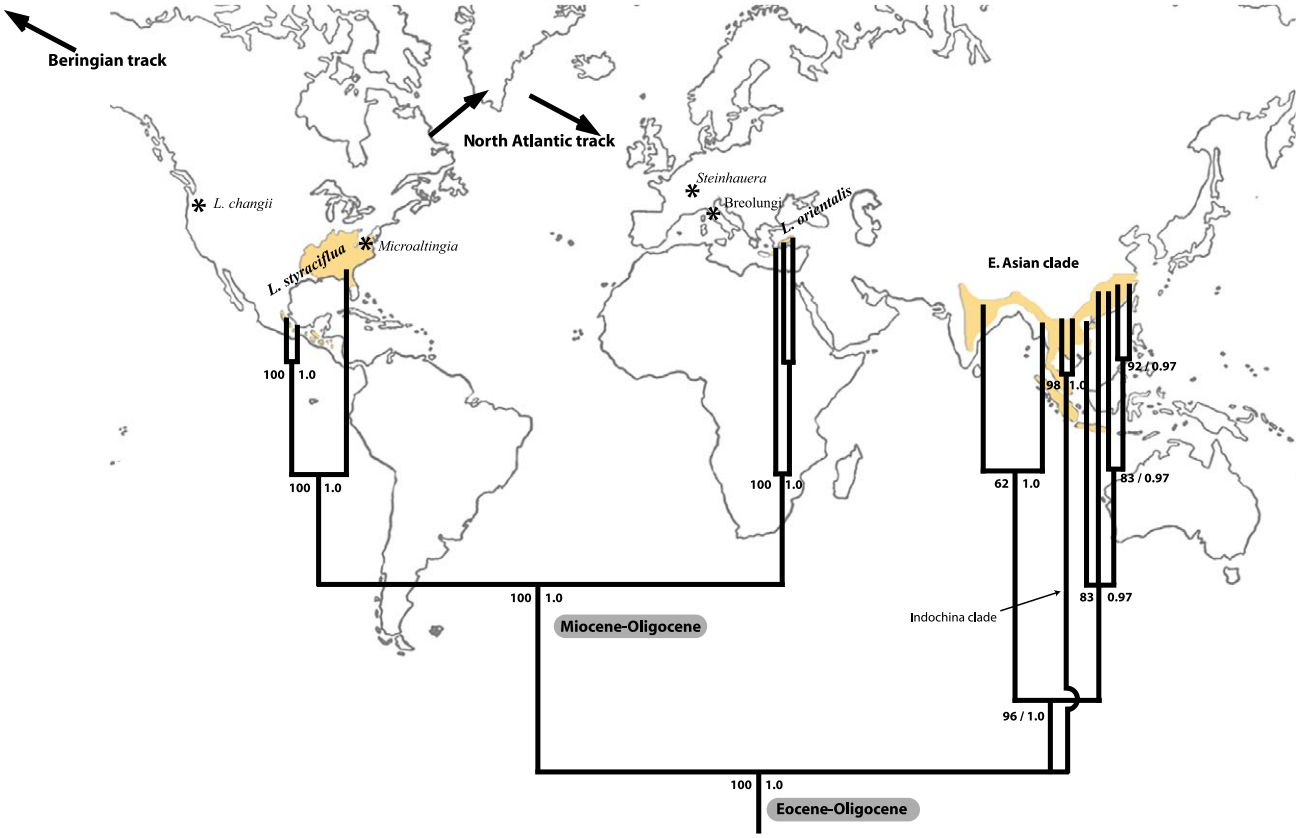

Fig. 5. Biogeographic diversification in Altingiaceae. Time estimates obtained for major splits within Altingiaceae from both PL and BRC given in shaded boxes. Stars indicate the localities of fossils in Altingiaceae (*Liquidambar changii* = 15.6 mya, *Steinhauera* = ~50 mya, *Microaltingia* = 90 mya, Breolungi, NW Italy, *Liquidambar* sp. = 3 mya). Bootstrap values are given to the left of branches for clades resolved in strict consensus, to the right of branches are Bayesian posterior probabilities.

Table 4
Comparison divergence times estimation from penalized likelihood and Bayesian analyses for all nodes ± 95% confidence intervals

Clade name	PL	Bayesian
17[a]	10.91 ± 3.31	22.90 ± 10.24 (3.58– 43.00)
18	3.69 ± 2.59	9.07 ± 5.76 (0.47–21.00)
19	15.60 ± 0.00	19.54 ± 3.63 (15.71–28.79)
20	17.52 ± 3.23	24.26 ± 5.21 (16.83–36.47)
21	18.87 ± 3.31	28.57 ± 6.11 (18.98–42.11)
22	20.38 ± 2.81	33.69 ± 6.87 (22.00–48.19)
23[b]	22.70 ± 3.17	39.12 ± 7.37 (25.57–54.03)
24	43.30 ± 5.18	72.77 ± 4.85 (61.68–80.61)
25	30.03 ± 5.22	46.07 ± 9.20 (27.42–63.10)
26	33.08 ± 8.24	33.21 ± 15.32 (3.97–60.31)
27	49.00 ± 3.44	61.19 ± 5.77 (50.68–72.30)
28	85.00 ± 0.00	85.41 ± 0.39 (85.01–86.46)
29	88.14 ± 0.40	86.26 ± 0.74 (85.19–88.01)
30	88.97 ± 0.33	87.30 ± 0.93 (85.64–89.15)
31	87.12 ± 0.37	89.05 ± 0.58 (87.67–89.87)
32	90 ± 0.00	89.58 ± 0.39 (88.56–89.99)

See Fig. 3 for position of node numbers. Nodes of biogeographic ineterest in Altingiaceae.

[a] Intercontinental disjunction between eastern N. America and western Asia.

[b] Divergence of eastern Asian clade from eastern N. America and western Asian clade.

4. Discussion

4.1. Monophyly of Altingiaceae

Our results from combined analysis of five non-coding regions confirm the monophyly of Altingiaceae (Shi et al., 1998, 2001) with strong support from all analyses (Figs. 1–5). Synapomorphies for the Altingiaceae include arborescent plants with (mostly) unisexual capitate spherical to turbinate pistillate inflorescences, bilocular capsules, septicidal, plus sometimes loculicidal dehiscence, many seeds per fruit, of which many are abortive, mature seeds with an encircling flange or distal wing (Bogle, 1986; Endress and Igersheim, 1999). This combination of characters is unique to Altingiaceae within the larger rosid clade (APG, 2003; Chase et al., 1993; Magallón et al., 1999; Soltis et al., 2000). After a relatively long period of independent evolution Altingiaceae appear to have radiated rather rapidly in the Tertiary (also see Ickert-Bond et al., 2005; Pigg et al., 2004), a process that left its signature in the short branches of the crown group (Fig. 2). Similar evolutionary scenarios have been proposed for the radiation of the South African Cape genus *Phylica* (Richardson et al., 2001) and for the myrtaceous Pennaeaceae and Oliniaceae (Schönenberger and Conti, 2003).

4.2. Paraphyly of Liquidambar

Our *cp*DNA results clearly show that *Liquidambar* is paraphyletic (Figs. 1–5). The data further corroborate the sister-group relationship between the western Asian *Liquidambar orientalis* and the eastern North American *L. styraciflua* that was already supported in previous phylogenetic analyses based on allozymes (Hoey and Parks, 1991, 1994) and DNA sequence data (Li et al., 1997a,b; Li and Donoghue, 1999; Shi et al., 1998; Shi et al., 2001). *Liquidambar macrophylla* Oersted from Central America, often considered conspecific with *L. styraciflua*, forms a very well supported clade with *L. styraciflua* from eastern North America (pp 1.0, BP = 100%). Morphologically, *L. macrophylla* has slightly larger leaves and fruits, and occurs in the cloud forests at high elevations (~1000–2300 m) in Mexico, Belize, El Salvador, Guatemala, Honduras, and Nicaragua as compared to *L. styraciflua* from eastern North America, which ranges from sea level to 300 m in elevation.

The other two species of *Liquidambar* (*L. acalycina* and *L. formosana*) appear in an eastern Asian clade along with *Altingia* and *Semiliquidambar* (Figs. 2 and 3). *Liquidambar acalycina* and *L. formosana* have been shown to form a well-supported clade (99% bootstrap) in a phylogenetic analysis of the four species of *Liquidambar* based on cp *mat*K sequences (Li et al., 1997a,b), as well as a combined analysis of ITS, *trn*L-trnF IGS, and GBSSI sequences (Li and Donoghue, 1999). With our expanded sampling of *Liquidambar* and other members of Altingiaceae, *L. formosana* and *L. acalycina* do not have a sister-species relationship. *Liquidambar acalycina* shared several morphological characters with *Liquidambar* (palmately-lobed, deciduous leaves and spinose extrafloral processes between adjacent fruits, and long, persistent styles, Ickert-Bond et al., 2005). Yet, it also has several similarities with *Altingia* including seeds with a circular flange (versus a distal wing in other species of *Liquidambar*), and broad carpel shapes (Ickert-Bond et al., 2005). We recently noted, that leaves of *L. acalycina* are highly variable similar to those of *Semiliquidambar*. These morphologies together with its non-monophyletic position in the phylogeny (Fig. 2) seem to suggest that morphologies of *L. acalycina* might have evolved from introgression. This hypothesis needs to be further tested with more extensive populational sampling of *L. acalycina*.

It is worth noting that *Liquidambar* was supported to be monophyletic in a morphological cladistic analysis (Ickert-Bond et al., 2005). Characters that support the monophyly of *Liquidambar* include long thin petioles, knob-like or spinose extrafloral processes, filaments that are longer than the anthers, and stomia on the anthers that bifurcate both distally and proximally. In addition persistent, straight styles, long thin peduncles on infructescences, and exserted fruits are characteristic of *Liquidambar*. The observed incongruence between the morphological and the molecular dataset might be due to convergence, reticulate evolution or lineage sorting (Doyle, 1992). The occurrence of extremely long filaments in the temperate *Liquidambar* as opposed to the very short stubby filaments in *Altingia*, might reflect different pollination syndromes in their respective habitats. Habitats in temperate forests of *Liquidambar* are open and long filaments aiding in wind pollination might be the preferred pollination syndrome, while subtropical habitats of *Altingia* are much more densely forested and pollination might involve insects as well, but detailed observation on pollination in *Altingia* are lacking (Vink, 1957). Additional characters of the anther, such as the stomium bifurcation in *Altingia* (both proximally and distally) and *Liquidambar* (none) might be related to differences in pollen presentation by these two genera (Hufford and Endress, 1989). We are continuing our detailed morphological and anatomical studies of *Altingia* to test the hypothesis that convergence has led to the data incongruence between molecules and morphology in Altingiaceae.

4.3. Polyphyly of widely distributed Altingia species

Two most widely distributed species of *Altingia* are *A. chinensis* and *A. gracilipes*, represented by several accessions both in our study from throughout their geographic range. These two taxa are both polyphyletic in our analysis, a condition that may be due to convergence, introgression, hybridization or incomplete lineage sorting (Funk and Olmland, 2003). Morphologically, *A. gracilipes* is highly distinct with small evergreen, coriaceous leaves, and small capitate infructescences with few fruits. There may be several cryptic species in this complex with such a combination of morphological characters. The molecular divergence of *A. gracilipes* correlates with the distribution of the populations throughout the geographic range.

Altingia chinensis forms a morphological complex with *A. obovata*, a taxon restricted to Hainan, which is recognized for its obovate leaves that are usually smaller than those of *A. chinensis*. Frequently, obovate leaves can be found in mainland China in populations of *A. chinensis*, and current taxonomy overestimates the significance of leaf morphology within a polymorphic *A. chinensis* complex. Similarly, Ferguson (1989) proposed to refer specimens formerly known as *A. poilanei* and *A. yunnanensis* under *A. chinensis*. Our results based on sequencing data do not corroborate this finding, since populations of *Altingia* from North Vietnam with leaf morphologies of *A. cf. poilanei* and *A. yunnanensis* are well supported as a distinct clade within Altingiaceae (pp 1.0, BP = 100%). Leaf margins of the North Vietnam and Yunnan populations appear strongly serrate as compared to the serrulate margin of most *A. chinensis* specimens surveyed (Ickert-Bond, unpublished).

4.4. Taxonomic implications

Morphological characters traditionally used to distinguish genera in Altingiaceae have focused on leaf shape, venation, and the presence or absence of spinose extrafloral structures between individual fruits in the infructescence

(Bogle, 1986; Chang, 1979; Endress, 1993; Ferguson, 1989; Ickert-Bond et al., 2005). Our molecular data show that the importance of these characters has been overemphasized and none of the three recognized "genera" is monophyletic. Our data suggest that Altingiaceae are best treated as consisting of one genus, *Liquidambar,* which has the nomenclatural priority over the two other generic names. Earlier workers (e.g., Bentham and Hooker, 1865; Blume, 1828; de Candolle, 1830; Lindley, 1836; Oken, 1841) also argued that the Altingiaceae should be united into one genus. Furthermore, infrageneric groupings as proposed by Chang (1959) and Harms (1930) for *Liquidambar* as well as those proposed for *Altingia* by Chang (1979) are not supported by our data (Fig. 2). A taxonomic synopsis of *Liquidambar s. l.*. is currently under preparation (S. Ickert-Bond and J. Wen, in prep.).

4.5. Historical biogeography

Hoey and Parks (1991) estimated the divergence times among species of *Liquidambar* based on isozyme data using Nei's (1987) and Thorpe's (1982) methods. *Liquidambar styraciflua* diverged ca. 7 mya (Nei's) or 13 mya (Thorpe's) from the Turkish *L. orientalis*, and 10 mya (Nei's) or 17 mya (Thorpe's) from the eastern Asian *L. formosana.* Our results from the Bayesian method date the divergence between the eastern North American *L. styraciflua* and the western Asian *L. orientalis* to be 23 ± 10.2 mya, or about 10 mya older than the previous estimates that were based on isozyme data (Fig. 4). The penalized likelihood method dates the same node with a divergence of 10.91 ± 3.3 mya, which is similar to the estimate based on isozyme data (Table 4). Donoghue et al. (2001) used a combined dataset of cp *mat*K, *trn*L, nr ITS, and *GBSSI* (waxy) sequences, and obtained 34.99 ± 5.5 mya for the eastern North American and western Asian intercontinental disjunction in *Liquidambar*. This considerably older estimate is perhaps due to their constraint of the crown group of *Liquidambar* to be 55 mya based on fossil leaves and pollen from the Middle Eocene. The fossil used for this estimate may be substantially older than the age of the crown group (also see Magallón, 2004). In our analysis, we used the anatomically preserved middle Miocene *L. changii* (Pigg et al., 2004) to constrain the divergence of the clade (*L. acalycina* (*L. formosana–A. obvata*)) from the rest of the eastern Asian clade to be minimally 15.6 mya. *Liquidambar changii* showed close morphological and anatomical similarities with the extant eastern Asian *L. acalycina* (Ickert-Bond et al., 2005; Pigg et al., 2004). The stem lineage of Altingiaceae was constrained to minimally 90 mya old based on fossil inflorescences, fruits and pollen of *Microaltingia* (Zhou et al., 2001). Furthermore, we used multiple well-preserved fossils from the closely related Hamamelidaceae *s. str.*, and close relatives (e.g., Exbucklandiaceae, Rhodoleiaceae) as additional calibration points. Morphological similarity between the intercontinental disjunct *L. styraciflua* and *L. orientalis* in light of their early divergence in the Oligocene/Miocene based on our estimates may be explained by morphological stasis via convergence, as has been proposed for many animal congeners (Glor et al., 2003; Lee and Frost, 2002; Rocha-Olivares et al., 2001; Schubart et al., 2000) as well as some plant taxa (Hedin, 2001; Liston et al., 1989; McDaniel and Shaw, 2003; Parks and Wendel, 1990; Wen, 1999). The estimated divergence also coincides with the availability of a North Atlantic migration route in the Middle Miocene (Fig. 5), which has been proposed to be the migration route for several other temperate intercontinental disjuncts, such as *Nyssa* and *Cornus* (Wen, 1998, 1999, 2001).

The other divergence of biogeographic interest is between the large eastern Asian clade and the clade of the North American *L. styraciflua* and the western Asian *L. orientalis*. Divergence times for this node have not been previously addressed, however general estimates range from 90–45 mya (late Cretaceous to Eocene) for *Liquidambar* species based on the substitution rate of cp *mat*K (5.5×10^{-11} base per site per year; Li et al., 1997a,b). The Bayesian method dates the divergence between the large eastern Asian clade and the clade of *L. styraciflua–L. orientalis* to be 39 ± 7.4 mya, while estimates from penalized likelihood are at 22.7 ± 3.2 mya (Figs. 4 and 5). The Eocene (~45–50 mya) presence of the fossil infructescence *Steinhauera* from Germany, considered close to *Altingia*, is consistent with this estimate (Mai, 1968). The Middle Miocene *L. changii* (15.6 mya) from western North America is most closely related to a member of the eastern Asian clade, *L. acalycina* (Pigg et al., 2004). The close relationship between the western North American fossil and the eastern Asian extant *Liquidambar* underscores a migration across the Bering land bridge (Fig. 5). Further fossil evidence from the Cretaceous *Microaltingia* from eastern North America, which dates the divergence of the stem lineage of Altingiaceae, indicates another biogeographic exchange between eastern North America and tropical/subtropical Asia during the Cretaceous. The presence of *Liquidambar* fossils in the Pliocene of Italy (Martinetto, 1998) is consistent with the widespread occurrence of *Liquidambar* in Europe in the Tertiary and indicates that the present-day intercontinental disjunctions are due to glaciation events including the impact of the Pleistocene cooling in Europe (Wen, 1999). Together, the fossil evidence and the results from analyses presented here demonstrate the complexity of biogeographic migrations in the history of Altingiaceae (Fig. 5). Additional markers are needed to further resolve the dynamics of the biogeographic diversification in the large eastern Asian clade.

Results from divergence time estimation using relaxed molecular clock approaches in our study show that the estimates from PL and BRC are largely congruent (Table 4). However, there are a few nodes, which exhibit significant differences. For example, the node of *Rhodoleia* and *Exbucklandia* is inferred to have diverged at 43.30 (±5.18) mya (PL) compared to 72.77 (±4.85) mya (BRC); other examples are nodes 21, 22, 23, 24, and 25. Since both methods weigh a likelihood function by either the

roughness penalty (PL) or the prior distribution (BRC), the results should converge, which has been demonstrated by Bell and Donoghue (2005), while differences in divergence times have been noted by others (Bell et al., 2005). It has been postulated that the differences in divergence time estimates may be related to the sensitivity of the prior distribution in the BRC (Wiegman et al., 2003; Yang and Yoder, 2003). Regions with short branch lengths are often correlated with short times separating successive nodes and those of phylogenetic uncertainty (e.g., with low BS and pp) (Wiegman et al., 2003). The ages of nodes close to calibration points have been shown to be more stable (Yang and Yoder, 2003; Linder et al., 2005). This is supported by our study; for example, node 18 is close to the calibration point of the Middle Miocene fossil (F4 in Figs. 3 and 4) and it is estimated to be 3.69 ± 2.59 mya with PL, and to be 9.07 ± 5.76 mya with BRC. Similarly, node 26 is close to the calibration point of the Lower Eocene fossil (~50 mya, F1 in Figs. 3 and 4) and is estimated to be 33.08 ± 8.24 mya (PL) versus 33.21 ± 15.32 mya with BRC.

4.6. Phylogenetic utility of non-coding plastid DNA in Altingiaceae

The five plastid regions used in our analysis, particularly the *trn*S-*trn*G IGS and the *trn*G intron, showed a set of characteristics similar to those reported by Kelchner (2002) for non-coding plastid regions, such as large strings of mononucleotides and small tandem repeats. All taxa have a poly A/T run of 10–15 bp in the *trn*G intron towards the 3′ end that prevents sequencing from that direction, possibly due to slipped-stranded mispairing of the two strands of the DNA double helix (Levinson and Gutman, 1987). The *trn*S-*trn*G-*trn*G fragment showed the highest phylogenetic utility at resolving species-level relationships in Altingiaceae, with 1.66% parsimony informative characters for the *trn*S-*trn*G IGS and 2.19% for the *trn*G intron. These results are comparable to a survey of the phylogenetic utility of 21 non-coding chloroplast markers (Shaw et al., 2005), nine non-coding regions in *Glycine*, Fabaceae (Xu et al., 2000) and five non-coding regions in Sinningieae, Gesneriaceae (Perret et al., 2003). In contrast, within four families of the Myrtales the *trn*S-*trn*G IGS contained fewer parsimony informative sites than *rps*16 and *rpL*16, but had more parsimony informative sites than *trn*H-*psb*A IGS, *atp*B-*rbc*L IGS and part of the *mat*K exon (Schönenberger and Conti, 2003). The occurrence of large poly A/T runs in both the *trn*S-*trn*G IGS and the *trn*G intron makes this marker costly to sequence for Altingiaceae, requiring at least five sequencing primers to recover reasonable overlap of reads.

Acknowledgments

The authors thank Necmi Aksoy (ISTO), Randall C. Hitchin (Washington Park Arboretum, Seattle, Washington), and Elizabeth A. Widjaja (BO) for providing material for study, B. Chen (IBSC), Y.W. Lam (HK), Phan Ke Loc (HNU), P. Wan (HK), and K.Y. Yip (HK) for assistance in the field, Ze Long Nie (KUN) for assistance with Bayesian divergence time estimation, the curators of the following herbaria for allowing access to collections A, ASU, E, F, FI, GH, HK, HN, K, IBSC, MO, P, PE, and XAL. Insightful comments by Kathleen Pigg, Martin Wojciechowski, and two annonymous reviewers greatly improved the content of the paper. This study was funded by the Pritzker Laboratory for Molecular Systematics and Evolution, a Boyd Postdoctoral Fellowship, a grant from the Field Dreams Program, Women's Board, (all Field Museum of Natural History), a National Geographic Society Explorers Grant NGS-7644-04, and a generous donation by the Wallace Desert Gardens, Scottsdale, Arizona (to S.M.I.-B.); and NSF DEB-0108536, and an Overseas Chinese Collaborative Research grant from the Chinese Academy of Sciences, to J.W.

References

Angiosperm Phylogeny Group (APG), 2003. An update of the Angiosperm Phylogeny Group classification for the orders and families of flowering plants AGPII. Bot. J. Linn. Soc. 141, 399–436.

Bell, C.D., Donoghue, M.J., 2005. Dating the Dipsacales: comparing models, genes, and evolutionary implications. Am. J. Bot. 92, 284–296.

Bell, C.D., Soltis, D.E., Soltis, P.S., 2005. The age of the angiosperms: a molecular timescale without a clock. Evolution 59, 1245–1258.

Bentham, G., Hooker, J.D., 1865. Genera Plantarum, vol. 1. Reeve, London, UK.

Blume, C.L., 1828. Flora Javae nec non insularum adjacentium. J. Frank, Brussels, Belgium.

Bogle, A.L., 1986. The floral morphology and vascular anatomy of the Hamamelidaceae: subfamily Liquidambaroideae. Ann. Mo. Bot. Gard. 73, 325–347.

Brandley, M.C., Schmitz, A., Reeder, T.W., 2005. Partitioned Bayesian analyses, partition choice, and the phylogenetic relationships of scincid lizards. Syst. Biol. 54, 373–390.

Bremer, B., Andreasen, K., Olsson, D., 1995. Subfamilial and tribal relationships in the Rubiaceae based on *rbc*L sequence data. Ann. Mo. Bot. Gard. 82, 383–397.

Buckley, T.R., 2002. Model misspecification and probabilistic test of topology: evidence from empirical data sets. Syst. Biol. 51, 509–523.

Buckley, T.R., Ahrensburger, P., Simon, C., Chambers, G.K., 2002. Combined data, Bayesian phylogenetics, and the origin of the New Zealand *Cicada* genera. Syst. Biol. 51, 4–18.

Bull, J.J., Huelsenbeck, J.P., Cunningham, C.W., Swofford, D.L., Waddell, P.J., 1993. Partioning and combining data in phylogenetic analyses. Syst. Biol. 42, 384–397.

Chang, H.-T., 1962. *Semiliquidambar*, novum Hamamelidacearum genus Sinicum. Sunyatsen University Bulletin of Natural Science 1, 34–44.

Chang, H.-T., 1973. A revision of the Hamamelidaceous flora of China. Bulletin of Sun-Yatsen University 1, 54–71.

Chang, H.-T., 1979. Hamamelidaceae. In: Chang, H.-T. (Ed.), Flora Reipublicae Popularis Sinicae, vol. 35, No. 2. Science Press, Beijing, China, pp. 36–116.

Chang, K.T., 1959. The pollen morphology of *Liquidambar* L. and *Altingia* Nor. Bot. Žurn. SSSR 44, 1375–1380.

Chang, T.-T., 1964. Pollen morphology of Hamamelidaceae and Altingiaceae. Acta Insituti Botanici Nomine V.L. Komarovii Academiae Scientiarum Unionis Rerum Publicarum Sovieticarum Socialisticarum, ser. 1, Flora et Systematica Plantae Vasculares 13, 173–232.

Chase, M.K., Soltis, D.E., Olmstead, R.G., Morgan, D., Les, D.H., Mischler, B.R., Duvall, M.R., Price, R.A., Hillis, H.G., Qiu, Y.-L., Kron, K.A., Rettig, J.H., Conti, E., Palmer, J.D., Manhart, J.R., Sytsma, K.J.,

Michaels, H.J., Kress, W.J., Karol, K.G., Clark, W.D., Hedrén, M., Gaut, B.S., Jansen, R.K., Kim, K.-J., Wimpee, C.F., Smith, J.F., Furnie, G.R., Strauss, S.H., Xiang, Q.-Y., Plunkett, G.M., Soltis, P.S., Swensen, S.M., Williams, S.E., Gadek, P.A., Quinn, C.J., Equiarte, L.E., Golenberg, L.E., Learn, G.H., Graham Jr., S.W., Barrett, S.C.H., Dayanandan, S., Albert, V.A., 1993. Phylogenetics of seed plants: an analysis of nucleotide sequences from the plastid gene *rbc*L. Ann. Mo. Bot. Gard. 80, 528–580.

Cronquist, A., 1981. An Integrated System of Classification of Flowering Plants. Columbia University Press, New York, USA.

Davis, C.C., Bell, C.D., Mathews, S., Donoghue, M.J., 2002. Laurasian migration explains Gondwanan disjunctions: evidence from Malpighiaceae. Proc. Natl. Acad. Sci. USA 99, 6833–6837.

de Candolle, A.P., 1830. Prodromus systematis naturalis regni vegetabilis. Treuttel et Würtz, Paris, France.

Donoghue, M.J., Bell, C.D., Li, J., 2001. Phylogenetic patterns in northern hemisphere plant geography. Int. J. Plant Sci. 162, S41–S52.

Doweld, A.B., 1998. Carpology, seed anatomy and taxonomic relationships of *Tetracentron* (Tetracentraceae) and *Trochodendron* (Trochodendraceae). Ann. Bot. (London) 82, 413–443.

Doyle, J.J., 1992. Gene trees and species trees: molecular systematics as one-character taxonomy. Syst. Bot. 17, 144–163.

Endress, P.K., 1989a. A suprageneric taxonomic classification of the Hamamelidaceae. Taxon 38, 371–376.

Endress, P.K., 1989b. Aspects of evolutionary differentiation of the Hamamelidaceae and the Lower Hamamelididae. Plant Syst. Evol. 162, 193–211.

Endress, P.K., 1989c. Phylogenetic relationships in the Hamamelidoideae. In: Crane, P.R., Blackmore, S. (Eds.), Evolution, systematics, and fossil history of the Hamamelidae, vol. 1, Systematics Association Special Volume No. 40A. Clarendon Press, Oxford, UK, pp. 227–248.

Endress, P.K., 1993. Hamamelidaceae. In: Kubitzki, K. (Ed.), The Families and Genera of Vascular Plants, vol. 2. Springer, New York, USA, pp. 322–331.

Endress, P.K., Igersheim, A., 1999. Gynoecium diversity and systematics of the basal eudicots. Bot. J. Linn. Soc. 130, 305–393.

Endress, P.K., Stumpf, S., 1990. The diversity of stamen structures in 'Lower' Rosidae (Rosales, Fabales, Proteales, Sapindales). Bot. J. Linn. Soc. 107, 217–293.

Felsenstein, J., 1985. Confidence limits on phylogenies: an approach using the bootstrap. Evolution 39, 783–791.

Felsenstein, J., 1988. Phylogenies from molecular sequences: inference and reliability. Annu. Rev. Genet. 22, 521–565.

Ferguson, D.K., 1989. A survey of the *Liquidambaroideae* (Hamamelidaceae) with a view to elucidating its fossil record. In: Crane, P.R., Blackmore, S. (Eds.), Evolution, Systematics, and Fossil History of the Hamamelidae, vol. 1, Systematics Association Special Volume No. 40A Clarendon Press, Oxford, UK, pp. 249–272.

Funk, D.J., Olmland, K.E., 2003. Species-level paraphyly and polyphyly: frequency, causes, and consequences, with insights from animal mitochondrial DNA. Annu. Rev. Ecol. Syst. 34, 397–423.

Glor, R.E., Kolbe, J.J., Powell, R., Larson, A., Lososi, J.B., 2003. Phylogenetic analyses of ecological and morphological diversification in Hispaniolan trunk-ground anoles (*Anolus cybotes* Group). Evolution 57, 2383–2397.

Goldman, N., Anderson, J.P., Rodrigo, A.G., 2000. Likelihood-based tests for topologies in phylogenetics. Syst. Biol. 49, 652–670.

Greguss, P., 1959. Holzanatomie der europäischen Laubhölzer und Sträucher. Akadémiai Kiadé, Budapest, Hungary.

Harms, H., 1930. Hamamelidaceae. In: Engler, A., Prantl, K. (Eds.), second ed. Die natürlichen Pflanzenfamilien, vol. 18a. Engelmann, Leipzig, Germany, pp. 303–343.

Hedin, M.C., 2001. Molecular insights into species phylogeny, biogeography, and morphological stasis in the ancient spider genus *Hypochilus* (Araneae: Hypochilidae). Mol. Phylogenet. Evol. 18, 238–251.

Herendeen, P.S., Magallón-Puebla, S., Lupia, R., Crane, P.R., Kobylinska, J., 1999. A preliminary conspectus of the Allon flora from the Late Cretaceous (Late Santonian) of central Georgia, USA. Ann. Mo. Bot. Gard. 86, 407–471.

Hoey, M.T., Parks, C.R., 1991. Isozyme divergence between eastern Asian, North American, and Turkish species of *Liquidambar* (Hamamelidaceae). Am. J. Bot. 78, 938–947.

Hoey, M.T., Parks, C.R., 1994. Genetic divergence in *Liquidambar styraciflua*, *L. formosana*, and *L. acalycina* (Hamamelidaceae). Syst. Bot. 19, 308–316.

Huang, G., 1986. Comparative anatomical studies on the woods of Hamamelidaceae in China. Acta Scientiarum Naturalium Universitatis Sunyatseni 1, 22–28.

Huang, Y.-L., Shi, S., 2002. Phylogenetics of Lythraceae sensu lato: a preliminary analysis based on chloroplast *rbc*L gene, *psa*A-*ycf*3 spacer, and nuclear rDNA internal transcribed spacer (ITS) sequences. Int. J. Plant Sci. 163, 215–225.

Huelsenbeck, J.P., Bull, J.J., 1996. A likelihood ratio test to detect conflicting phylogenetic signal. Syst. Biol. 45, 92–98.

Huelsenbeck, J.P., Ronquist, F.R., 2001. MrBayes: Bayesian inference of phylogenetic trees. Bioinformatics 17, 754–755.

Huelsenbeck, J.P., Ronquist, F.R., Nielsen, R., Bollback, J.P., 2001. Bayesian inference of phylogeny and its impacts on evolutionary biology. Science 294, 2310–2314.

Hufford, L., Crane, P.R., 1989. A preliminary phylogenetic analysis of the 'lower' Hamamelidae. In: Crane, P.R., Blackmore, S. (Eds.), Evolution, Systematics, and Fossil History of the Hamamelidae, vol. 1, Systematics Association Special Volume No. 40A Clarendon Press, Oxford, UK, pp. 175–192.

Hufford, L.D., Endress, P.K., 1989. The diversity of anther structure and dehiscence patterns among Hamamelididae. Bot. J. Linn. Soc. 99, 301–346.

Ickert-Bond, S.M., Pigg, K.B., Wen, J., 2005. Comparative infructescence morphology in *Liquidambar* (Altingiaceae) and its evolutionary significance. Am. J. Bot. 92, 1234–1255.

Jeanmougin, F., Thompson, J.D., Gouy, M., Higgins, D.G., Gibson, T.J., 1998. Multiple sequence alignment with ClustalX. Trends Biochem. Sci. 23, 403–405.

Kauff, F., Lutzoni, F., 2002. Phylogeny of the Gyalectales and Ostropales (Ascomycota, Fungi): among and within order relationships based on nuclear ribosomal RNA small and large subunits. Mol. Phylogenet. Evol. 25, 138–156.

Kelchner, S., 2002. Group II introns as phylogenetic tools: structure, function, and evolutionary constraints. Am. J. Bot. 89, 1651–1669.

Kishino, H., Hasegawa, M., 1989. Evaluation of the maximum likelihood estimate of the evolutionary tree topologies from DNA sequence data, and the branching order in Hominoidea. J. Mol. Evol. 29, 170–179.

Larget, B., Simon, D.L., 1999. Markov chain Monte Carlo algorithms for the Bayesian analysis of phylogenetic trees. Mol. Biol. Evol. 16, 750–759.

Lee, C.E., Frost, B.W., 2002. Morphological stasis in the *Eurytemora affinis* species complex (Copepoda: Temoridae). Hydrobiologia 480, 111–128.

Levinson, G., Gutman, G.A., 1987. Slipped-Strand mispairing: a major mechanism for DNA sequence evolution. Mol. Biol. Evol. 4, 203–221.

Lewis, P.O., 2001. Phylogenetic systematics turns over a new leaf. Trends Ecol. Evol. 16, 30–37.

Li, J., Bogle, A.L., Klein, A.S., 1997a. Interspecific relationships and genetic divergence of the disjunct genus *Liquidambar* (Hamamelidaceae) inferred from DNA sequences of plastid gene *mat*K. Rhodora 99, 229–240.

Li, J., Bogle, A.L., Klein, A.S., 1997b. Phylogenetic relationships of the Hamamelidaceae inferred from sequences of internal transcribed spacers (ITS) of nuclear ribosomal DNA. Am. J. Bot. 86, 1027–1037.

Li, J., Donoghue, M.J., 1999. More molecular evidence for interspecific relationships in *Liquidambar* (Hamamelidaceae). Rhodora 101, 87–91.

Linder, H.P., Hardy, C.R., Rutschmann, F., 2005. Taxon sampling effects in molecular clock dating: an example from the African Restionaceae. Mol. Phylogenet. Evol. 35, 569–582.

Lindley, J., 1836. A Natural System of Botany. Longman, London, Great Britain.

Liston, A., Rieseberg, L.H., Elias, T., 1989. Morphological stasis and molecular divergence in the intercontinental disjunct genus *Datisca* (Datiscaceae). Aliso 12, 525–542.

Lumbsch, H.T., Schmitt, I., Palice, Z., Wiklund, E., Ekman, S., Wedin, M., 2004. Supraordinal phylogenetic relationships of the Lecanoromycetes based on a Bayesian analyses of combined nuclear and mitochondrial sequences. Mol. Phylogenet. Evol. 31, 822–832.

Magallón, S., 2004. Dating lineages: molecular and paleontological approaches to the temporal framework of clades. Int. J. Plant Sci. 165, S7–S21.

Magallón, S., Sanderson, M.J., 2005. Angiosperm divergence times: the effect of genes, codon positions, and time constraints. Evolution 59, 1653–1670.

Magallón, S., Crane, P.R., Herendeen, P.S., 1999. Phylogenetic pattern, diversity, and diversification of eudicots. Ann. Mo. Bot. Gard. 86, 297–372.

Magallón, S., Crane, P.R., Herendeen, P.S., 2001. *Androdecidua endressii*, gen. et sp nov., from the Late Cretaceous of Georgia (United States): further floral diversity in Hamamelidoideae (Hamamelidaceae). Int. J. Plant Sci. 162, 963–983.

Mai, D.H., 1968. Zwei ausgestorbene Gattungen im Tertiär Europas und ihre florengeschichtliche Bedeutung. Palaeontographica 123B, 184–199.

Manchester, S.R., 1999. Biogeographical relationships of North American Tertiary floras. Ann. Mo. Bot. Gard. 86, 472–522.

Martinetto, E., 1998. East Asian elements in the Plio-Pleistocene floras of Italy. In: Zhang, A., Sugong, W. (Eds.), Proceedings of the International Symposium of Floristic Characteristics and Diversity of East Asian Plants. Springer, Berlin, Germany, pp. 71–87.

McDaniel, S.F., Shaw, J., 2003. Phylogeographic structure and cryptic speciation in the trans-antarctic moss *Pyrrhobryum mnioides*. Evolution 57, 205–215.

Metcalfe, F.P., Chalk, L., 1950. Anatomy of Dicotyledons. Clarendon Press, Oxford, UK.

Meyer, F.G., 1993. Hamamelidaceae. In: Flora of North America North of Mexico, vol. 3, Flora of North America Editorial Committee Oxford University Press, New York, USA, pp. 362–367.

Moll, J.W., Janssonius, H.H., 1914. Mikrographie des Holzes der auf Java vorkommenden Holzarten III. E.J. Brill, Leiden, The Netherlands.

Nei, M., 1987. Molecular evolutionary genetics. Columbia University Press, New York.

Nylander, J.A.A., Ronquist, F., Huelsenbeck, J.P., Nieves-Aldrey, J.L., 2004. Bayesian phylogenetic analysis of combined data. Syst. Biol. 53, 47–67.

Oken, L., 1841. Allgemeine Naturgeschichte für alle Stände 3 (3): 1539. Hoffman'sche Verlagsbuchhandlung, Stuttgart, Germany.

Oxelman, B., Lidén, M., Berglund, D., 1997. Chloroplast *rps*16 intron phylogeny of the tribe Sileneae (Caryophyllaceae). Plant Syst. Evol. 206, 393–410.

Parks, C.R., Wendel, J.F., 1990. Molecular divergence between Asian and North American species of *Liriodendron* (Magnolicaceae) with implications of fossil floras. Am. J. Bot. 77, 1243–1256.

Pereira, S.L., Baker, A.J., 2004. Vicariant speciation of curassows (*Aves*, *Cracidae*): a hypothesis based on mitochondrial DNA phylogeny. The Auk 121, 682–694.

Perret, M., Chautems, A., Spichiger, R., Kite, G., Salvolainen, V., 2003. Systematics and evolution of tribe Sinningieae (Gesneriaceae): evidence from phylogenetic analyses of six plastid DNA regions and nuclear *ncpGS*. Am. J. Bot. 90, 445–460.

Pigg, K.B., Ickert-Bond, S.M., Wen, J., 2004. Anatomically preserved *Liquidambar* (Altingiaceae) from the Middle Miocene of Yakima Canyon, Washingon State, USA, and its biogeographic implications. Am. J. Bot. 91, 499–509.

Posada, D., Crandall, K.A., 1998. MODELTEST: testing the model of DNA substitution. Bioinformatics 14, 817–818.

Radtke, M.G., Pigg, K.B., Wehr, W.C., 2005. Fossil *Corylopsis* and *Fothergilla* leaves (Hamamelidaceae) from the Lower Eocene flora of Republic, Washington, USA, and their evolutionary and biogeographic significance. Int. J. Plant Sci. 166, 347–356.

Rambaut, A., Grassly, N.C., 1997. Seq-Gen: an application for the Monte Carlo simulation of DNA sequence evolution along phylogenetic trees. Comput. Appl. Biosci. 13, 235–238.

Rao, K.R., Purkayastha, S.K., 1972. In: Indian woods. Their identification, properties and uses, vol. 3. Forest Research Institute, Dehra Dun, India.

Reeder, T.W., 2003. A phylogeny of the Australian *Sphenimophus* group (*Scincidae: Squamata*) and the phylogenetic placement of the crocodile skinks (*Tribolontus*): Bayesian approaches to assessing congruence and obtaining confidence in maximum likelihood inferred relationships. Mol. Phylogenet. Evol. 27, 384–397.

Reinsch, A., 1890. Über die anatomischen Verhältnisse der Hamamelidaceae mit Rücksicht auf ihre systematische Gruppierung. Bot. Jahrb. Syst. 11, 347–395.

Richardson, J.E., Weitz, F.M., Fay, M.F., Cronk, Q.C.B., Linder, H.P., Reeves, G., Chase, M.W., 2001. Rapid and recent origin of species richness in the cape flora of South Africa. Nature 412, 181–183.

Rocha-Olivares, A., John, W., Fleeger, J.W., Foltz, D.W., 2001. Decoupling of molecular and morphological evolution in deep lineages of a meiobenthic harpacticoid copepod. Mol. Biol. Evol. 18, 1088–1102.

Sanderson, M.J., 1997. A non-parametric approach for estimating divergence times in the absence of rate constancy. Mol. Biol. Evol. 14, 1218–1231.

Sanderson, M.J., 2002. Estimating absolute rates of molecular evolution and divergence times: a penalized likelihood approach. Mol. Phylogenet. Evol. 19, 101–109.

Sanderson, M.J., 2003. r8s: inferring absolute rates of molecular evolution and divergence times in the absence of a molecular clock. Bioinformatics 19, 301–302.

Schönenberger, J., Conti, E., 2003. Molecular phylogeny and floral evolution of Penaeaceae, Oliniaceae, Rhynchocalycaceae, and Alzateaceae (Myrtales). Am. J. Bot. 90, 293–309.

Schubart, C.D., Neigel, J.E., Felder, D.L., 2000. Molecular biology of mud crabs (Brachyura: Panopeidae) from the northwestern Atlantic and the role of morphological stasis and convergence. Mar. Biol. 137, 11–18.

Shaw, J., Lickey, E.B., Beck, J.T., Farmer, S.B., Liu, W., Miller, J., Siripun, K.C., Winder, C.T., Schilling, E.E., Small, R.L., 2005. The tortoise and the hare II: relative utility of 21 noncoding chloroplast DNA sequences for phylogenetic analysis. Am. J. Bot. 92, 142–166.

Shi, S., Chang, H.-T., Chen, Y., Qu, L., Wen, J., 1998. Phylogeny of the Hamamelidaceae based on the ITS sequences of nuclear ribosomal DNA. Biochem. Syst. Ecol. 26, 55–69.

Shi, S., Huang, Y., Zhong, Y., Du, Y., Zhang, Q., Chang, H., Boufford, D.E., 2001. Phylogeny of the Altingiaceae based on cpDNA *mat*K, PY-IGS and nrDNA ITS sequences. Plant Syst. Evol. 230, 13–24.

Simoes, A.O., Endress, M.E., van der Niet, T., Kinoshita, L.S., Conti, E., 2004. Tribal and intergeneric relationships of Mesechiteae (Apocynoideae, Apocynaceae): evidence from three noncoding plastid DNA regions and morphology. Am. J. Bot. 91, 1409–1418.

Soltis, D.E., Soltis, P.S., Chase, M.W., Mort, M.E., Albach, T.D., Zanis, M., Savolaninen, V., Hahn, W.H., Hoot, S.B., Fay, M.F., Axtell, M., Swensen, S.M., Prince, L.M., Kress, W.J., Nixon, K.C., Farris, J.S., 2000. Angiosperm phylogeny inferred from 18S rDNA, *rbc*L, and *atp*B sequences. Bot. J. Linn. Soc. 133, 381–461.

Sosa, V., 1978. Hamamelidaceae. In: Gómez-Pompa, A., Sosa, V. (Eds.), Flora of Veracruz. Fasc., vol. 1. Instituto de Investigaciones sobre Recursos Bioticos, A.C. Xalapa, Veracruz, Mexico, pp. 1–50.

Swofford, D.I., 2002. PAUP*. Phylogenetic Analysis Using Parsimony (* and Other Methods). Version 4. Sinauer Associates, Sunderland, Massachusetts, USA.

Swofford, D.I., Olsen, G.J., Waddell, P.J., Hillis, D.M., 1996. Phylogenetic inference. In: Hillis, D.M., Moritz, C., Mable, B.K. (Eds.), Mol. Syst.. Sinauer Associates, Sunderland, Massachusetts, USA, pp. 407–514.

Taberlet, P., Gielly, L., Pantaou, G., Bouvet, J., 1991. Universal primers for amplification of three non-coding regions of chloroplast DNA. Plant Mol. Biol. 17, 1105–1109.

Tang, Y., 1943. Systematic anatomy of the woods of the Hamamelidaceae. Bull. Fan Mem. Inst. Biol. (New Series) vol. 1, 8–63.

Thorpe, J.P., 1982. The molecular clock hypothesis: biochemical evolution, genetic differentiation and systematics. Annu. Rev. Ecol. Syst. 13, 139–410.

Thorne, J.L., Kishino, H., 2002. Divergence time and evolutionary rate estimation with multilocus data. Syst. Biol. 51, 689–702.

Thorne, J.L., Kishino, H., Painter, I.S., 1998. Estimating the rate of evolution of the rate of molecular evolution. Mol. Biol. Evol. 15, 1647–1657.

Tippo, O., 1938. Comparative anatomy of the Moraceae and their presumed allies. Bot. Gaz. 100, 1–99.

Vink, W., 1957. Hamamelidaceae. In: van Steenis, C.G.G.J. (Ed.), Flora Malesiana, 5. The Nationaal Herbarium Nederland, Leiden, The Netherlands, pp. 363–379.

Wen, J., 1998. Evolution of the eastern Asian and eastern North American disjunct pattern: insights from phylogenetic studies. Korean J. Plant Taxon. 28, 63–81.

Wen, J., 1999. Evolution of eastern Asian and eastern North American disjunct distributions in flowering plants. Annu. Rev. Ecol. Syst. 30, 421–455.

Wen, J., 2001. Evolution of eastern Asian-eastern North American biogeographic disjunctions: a few additional issues. Int. J. Plant Sci. 162, S117–S122.

Wiegman, B.M., Yeates, D.K., Thorne, J.L., Kishino, H., 2003. Time flies, a new molecular time-scale for brachyceran fly evolution without a clock. Syst. Biol. 52, 745–756.

Wisniewski, M., Bogle, A.L., 1982. The ontogeny of the inflorescence and flower of *Liquidambar styraciflua* L. (Hamamelidaceae). Am. J. Bot. 69, 1612–1624.

Wolfe, J.A., 1973. Fossil forms of the Amentiferae. Brittonia 25, 334–355.

Xu, D.H., Abe, J., Sakai, M., Kanazawa, A., Shimamoto, Y., 2000. Sequence variation of non-coding regions of chloroplast DNA of soybean and related wild species and its implications for the evolution of different chloroplast haplotypes. Theor. Appl. Genet. 101, 724–732.

Yang, Z., 1997. PAML: A program package for phylogenetic analysis by maximum likelihood. CABIOS 13, 555–556.. Available from: http://abacus.gene.ucl.ac.uk/software/paml.html.

Yang, Z., Yoder, A.D., 2003. Comparison of likelihood and Bayesian methods for estimating divergence times using multiple gene loci and calibration points, with application to a radiation of cute-looking mouse lemur species. Syst. Biol. 52, 705–716.

Zavada, M.S., Dilcher, D.L., 1986. Comparative pollen morphology and its relationship to phylogeny of pollen in the Hamamelidae. Ann. Mo. Bot. Gard. 73, 348–381.

Zhou, Z.W., Crepet, W.L., Nixon, K.C., 2001. The earliest fossil record of the Hamamelidaceae: Late Cretaceous (Turonian) inflorescences and fruits of Altingioideae. Am. J. Bot. 88, 753–766.